NASA/TM—2012-217128

Alternate-Fueled Combustor-Sector Performance

Part A: Combustor Performance

Part B: Combustor Emissions

D.T. Shouse and C. Neuroth
Air Force Research Laboratory, Wright-Patterson Air Force Base, Dayton, Ohio

R.C. Hendricks
Glenn Research Center, Cleveland, Ohio

A. Lynch, C.W. Frayne, J.S. Stutrud, E. Corporan, and Capt. T. Hankins
Air Force Research Laboratory, Wright-Patterson Air Force Base, Dayton, Ohio

July 2012

NASA STI Program . . . in Profile

Since its founding, NASA has been dedicated to the advancement of aeronautics and space science. The NASA Scientific and Technical Information (STI) program plays a key part in helping NASA maintain this important role.

The NASA STI Program operates under the auspices of the Agency Chief Information Officer. It collects, organizes, provides for archiving, and disseminates NASA's STI. The NASA STI program provides access to the NASA Aeronautics and Space Database and its public interface, the NASA Technical Reports Server, thus providing one of the largest collections of aeronautical and space science STI in the world. Results are published in both non-NASA channels and by NASA in the NASA STI Report Series, which includes the following report types:

- TECHNICAL PUBLICATION. Reports of completed research or a major significant phase of research that present the results of NASA programs and include extensive data or theoretical analysis. Includes compilations of significant scientific and technical data and information deemed to be of continuing reference value. NASA counterpart of peer-reviewed formal professional papers but has less stringent limitations on manuscript length and extent of graphic presentations.

- TECHNICAL MEMORANDUM. Scientific and technical findings that are preliminary or of specialized interest, e.g., quick release reports, working papers, and bibliographies that contain minimal annotation. Does not contain extensive analysis.

- CONTRACTOR REPORT. Scientific and technical findings by NASA-sponsored contractors and grantees.

- CONFERENCE PUBLICATION. Collected papers from scientific and technical conferences, symposia, seminars, or other meetings sponsored or cosponsored by NASA.

- SPECIAL PUBLICATION. Scientific, technical, or historical information from NASA programs, projects, and missions, often concerned with subjects having substantial public interest.

- TECHNICAL TRANSLATION. English-language translations of foreign scientific and technical material pertinent to NASA's mission.

Specialized services also include creating custom thesauri, building customized databases, organizing and publishing research results.

For more information about the NASA STI program, see the following:

- Access the NASA STI program home page at *http://www.sti.nasa.gov*

- E-mail your question via the Internet to *help@sti.nasa.gov*

- Fax your question to the NASA STI Help Desk at 443–757–5803

- Telephone the NASA STI Help Desk at 443–757–5802

- Write to:
  NASA Center for AeroSpace Information (CASI)
  7115 Standard Drive
  Hanover, MD 21076–1320

NASA/TM—2012-217128

Alternate-Fueled Combustor-Sector Performance
Part A: Combustor Performance
Part B: Combustor Emissions

D.T. Shouse and C. Neuroth
Air Force Research Laboratory, Wright-Patterson Air Force Base, Dayton, Ohio

R.C. Hendricks
Glenn Research Center, Cleveland, Ohio

A. Lynch, C.W. Frayne, J.S. Stutrud, E. Corporan, and Capt. T. Hankins
Air Force Research Laboratory, Wright-Patterson Air Force Base, Dayton, Ohio

National Aeronautics and
Space Administration

Glenn Research Center
Cleveland, Ohio 44135

July 2012

This work was sponsored by the Fundamental Aeronautics Program
at the NASA Glenn Research Center.

Level of Review: This material has been technically reviewed by technical management.

Available from

NASA Center for Aerospace Information
7115 Standard Drive
Hanover, MD 21076–1320

National Technical Information Service
5301 Shawnee Road
Alexandria, VA 22312

Available electronically at http://www.sti.nasa.gov

Alternate-Fueled Combustor-Sector Performance
Part A: Combustor Performance
Part B: Combustor Emissions

D.T. Shouse and C. Neuroth
Air Force Research Laboratory
Wright-Patterson Air Force Base
Dayton, Ohio 45433

R.C. Hendricks
National Aeronautics and Space Administration
Glenn Research Center
Cleveland, Ohio 44135

A. Lynch, C.W. Frayne, J.S. Stutrud, E. Corporan, and Capt. T. Hankins
Air Force Research Laboratory
Wright-Patterson Air Force Base
Dayton, Ohio 45433

Abstract

Alternate aviation fuels for military or commercial use are required to satisfy MIL-DTL-83133F(2008) or ASTM D 7566 (2010) standards, respectively, and are classified as "drop-in" fuel replacements. To satisfy legacy issues, blends to 50% alternate fuel with petroleum fuels are certified individually on the basis of processing and assumed to be feedstock agnostic. Adherence to alternate fuels and fuel blends requires "smart fueling systems" or advanced fuel-flexible systems, including combustors and engines, without significant sacrifice in performance or emissions requirements. This paper provides preliminary performance (Part A) and emissions and particulates (Part B) combustor sector data. The data are for nominal inlet conditions at 225 psia and 800 °F (1.551 MPa and 700 K), for synthetic-paraffinic-kerosene- (SPK-) type (Fisher-Tropsch (FT)) fuel and blends with JP-8+100 relative to JP-8+100 as baseline fueling. Assessments are made of the change in combustor efficiency, wall temperatures, emissions, and luminosity with SPK of 0%, 50%, and 100% fueling composition at 3% combustor pressure drop. The performance results (Part A) indicate no quantifiable differences in combustor efficiency, a general trend to lower liner and higher core flow temperatures with increased FT fuel blends. In general, emissions data (Part B) show little differences, but with percent increase in FT-SPK-type fueling, particulate emissions and wall temperatures are less than with baseline JP-8. High-speed photography illustrates both luminosity and combustor dynamic flame characteristics.

Introduction

Synthetic and biomass fueling are now considered as near-term aviation alternate fueling. The major impediment is a secure sustainable supply of these fuels at reasonable cost. Alternate aviation fuels are currently required to satisfy MIL-DTL-83133F (2008) for Fisher-Tropsch- (FT-) equivalent processed ASTM D 7566 (2010) and known as "drop-in" fuel replacements (military and civil, respectively). As in aviation, many land-based and marine power generation systems are elderly, known as the legacy issue. Fueling these systems requires careful compliance to the fuel handling and engine systems for which they were (are) designed. To satisfy a sustainable fuel supply, it will be necessary to accept fuels derived from a variety of feedstocks. Consequently, adherence to alternate fuels and fuel blends requires "smart fueling

systems" or advanced fuel-flexible systems, including combustors and engines, without significant sacrifice in performance or emissions requirements.

The common military services fueling concept is that JP-8+100 or alternate FT-type fuels that can fuel gas turbines as well as many diesel systems. Diesel biomass-derived oils are often unsuitable because sufficient aromatics and sulfur are lacking, which provide lubricity, thus reducing design component life. To counter these issues, additives are promoted.

This paper provides preliminary performance, luminosity, emissions, and particulates combustor sector data relative to JP-8+100 as baseline fueling, for synthetic-parafinic-kerosene- (SPK-) type fuel blends (herein FT-type fuel) and projections for testing of biofuel fuel blends leading to preliminary development of smart fueling (fuel flexible) and combustor systems for the next generation aeronautic and aeronautic-derivative gas turbine engines. Fuel flexibility is an engine operations goal to enable various designer fuels operations with minor alterations in controller function or geometry.

Truly performance and emissions are coupled issues; however, combustor performance will be presented in Part A and combustor emissions as Part B for understanding both in sufficient detail. Herein, fueling acronyms are synthetic paraffinic kerosene (SPK), and hydro-treated renewable jet (HRJ) also known as bio-SPK or SPK-HEFA (SPK from hydroprocessed esters and fatty acids) and proposed as ASTM D7566-Annex-1.

Part A: Combustor Performance

Part A presents fueling characteristics, facility development, and operation followed by thermal performance of the combustor and combustor visualization. The results are for one of several combustors—herein denoted as combustor A—to be evaluated in development of fuel-flexible engine combustors.

Most data herein are testing at nominal inlet conditions of 225 psia and 800 °F (1.55 MPa, 700 K) at 3% combustor pressure drop, where JP-8+100 (JP-8) is taken as baseline. Selected emissions data are provided at and below 225 psia (1.55 MPa).

Fuel Characteristics

In general all alternate fueling is required to meet or exceed MIL-DTL-83133F or ASTM D7566 and Annex 1 requirements. The carbon-distribution for each fuel used and primary characteristics differ depending on feedstock source and distilling practices, yet all fall within specification. Typical C-distributions for JP-8 and an (SPK) FT-derived fuel are shown in Figure 1(a) with vendor variations in fuels illustrated in Figure 1(b). Secondary refining of petroleum-based kerosene fuels can also satisfy specifications.

The specifications for one of the fuels, AFRL No. 5172 Shell GTL-SPK (FT), are presented in Appendix A.

While fuels purchased by Defense Energy Support Center (DESC) are within specification, independent of whether petroleum- or alternate-based fuels, batch-to-batch variations do occur depending on processors, feedstock, ;production date and location of fuel production: a world-wide fuels sourcing problem.

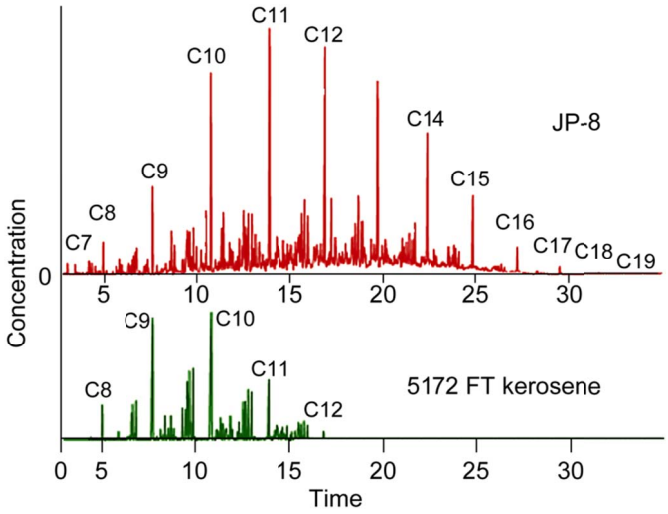

Figure 1(a).—Representative carbon distributions for JP-8 and AFRL No. 5172 FT (SPK) from Shell gas-to-liquid (GTL) with 0% aromatics and 0% sulfur. The JP-8 cited is 19% aromatics and 1200 ppm sulfur.

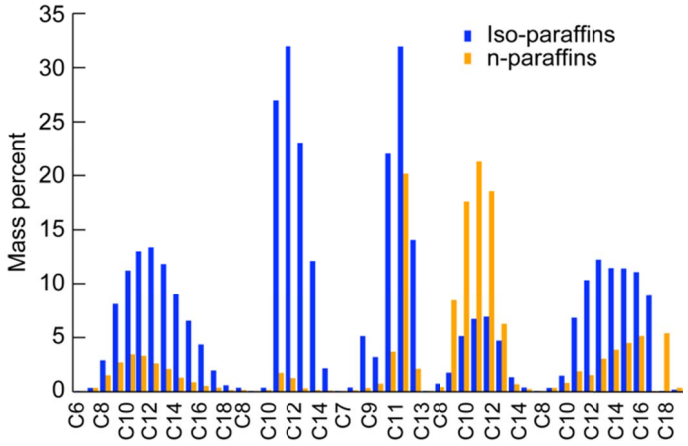

Figure 1(b).— Variations in representative carbon distributions for proposed alternate fuels with high and low n-paraffinic to isomer ratios.

Combustor and Facility Characteristics

The general description of the combustor and supporting research cell data are similar to those reported in Hendricks et al. (Ref. 1). The particular aspects of the geometry tested are proprietary and will not be discussed herein. Details of the High Pressure Combustion Research Facility at the Air Force Research Laboratory (AFRL) are provided by Shouse et al. (Ref. 2).

Although some general aspects of the fuel delivery system and operations of the facility are similar to those of References 1 and 2, specific facility modifications and increased capability to handle fuel blending had to be made, including remote alternate test fuel storage/tankage and delivery of the alternate test fuel to the facility fuel pumps, flow meters, and control systems (see Appendix B).

Facility Development

Before validation data could be taken, it was necessary to learn what it takes to conduct high-pressure combustor testing of alternate fuels such as FT and biomass feedstock fuels. It is first necessary to establish the combustion parameters required by the study such as operability, performance, durability time-dependent measurements such as flame studies, and others. Next, an assessment of the effects of pressure ratios and inlet temperatures on both the combustor sector model and desired data was undertaken as well as most importantly, how to safely blend the fuels. The blending system, while complex, enables operations to establish and stabilize combustor inlet pressures and temperatures of preheated air at the required test condition without the additional complication of simultaneously establishing fuel blend.

To establish the fuel delivery system, questions such as how much fuel and time are required to fully evaluate a typical fuel candidate must be resolved. A 500-gal trailer-mounted fuel tank was chosen for porting alternative fuels with the added feature of coupling to the facility fueling system. The facility has two duplicate fuel systems that provided a means of handling JP-8 fuel with one system to pump, meter, and control the JP-8 fuel; this system is referred to as the main fuel delivery system. The identical system was fed the alternative fuel supply, which is pumped from the trailer into the facility primary fuel system and ultimately blended online with the main fuel system to provide the desired fuel blend from 0% to 100% trailer fuel. An analysis of fuel blending errors is provided in Appendix C. To verify the 50/50 blend, samples were collected just upstream of the fuel injectors and analyzed using liquid chromatography; blending is within ±4%.

Test Parameters and Data Collection

For this series of testing, the nominal test conditions for pressures and temperatures of blends and the extensive data collection systems have been established. The parameters were chosen to be most representative of engine operations envelope from idle to altitude cruise; however, TO (take-off) pressures are currently beyond the range of this facility.

Combustor parameters
Inlet pressures (P): 75, 125, 175, and 225 psia (0.517, 0.862, 1.207, and 1.551 MPa)
Inlet temperature (T): 500, 625, 725, and 790 °F (533, 603, 658, and 694 K)
Combustor pressure drops (ΔP): 3%, 4%, and 5%
Fuel blends: 100% JP-8, 50:50 JP-8:FT, and 100% FT

Data collection
Gaseous emissions
Exit temperature rake type B thermocouples, (also for metal and sidewall temperatures)
Photo diode output (voltage)
Still and high-speed photography
Smoke and particulate emissions

Combustor outer and inner liner temperature data are given in Appendix D, and estimates of errors in performance, flame temperature, emissions data, and geometric coordinates are given in Appendix C.

Combustor Thermal Performance

The combustion efficiencies for combinations of fuel:air ratio F/A and fuel compositions were of the order of 99.9% (Table 1), and one is unable to distinguish combustor changes from this single parameter; thus, other parameters will be investigated. For example, the emissions-based calculated flame

TABLE 1.—VARIATIONS IN COMBUSTOR EFFICIENCIES WITH F/A AND FUELING COMPOSITION FOR NOMINAL INLET CONDITIONS AT 225 PSIA (1.551 MPA) AND 800 °F (700 K) WITH JP-8 +100 AS BASELINE.[a] COMBUSTOR PRESSURE DROP ~3%

F/A	JP-8 +100	JP-8:FT 50:50 blend	FT
	F	H	G
0.010	99.89	99.9	99.91
	O	K	M
0.015	99.93	99.94	99.91
	Q	U	T
0.020	99.94	99.94	99.95
0.025			

[a]Letters refer to proprietary data reduction parameters.

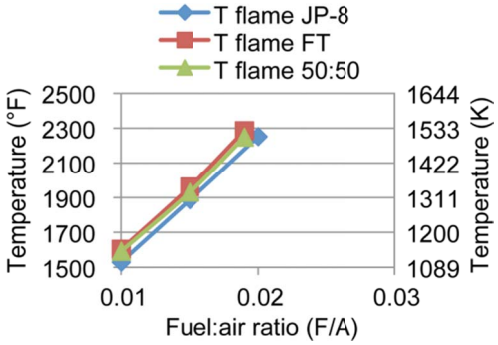

Figure 2.—Calculated flame temperature variation with F/A and fuel composition.

temperature (Fig. 2), increases with F/A, with FT about $\Delta T = 70$ °F (39 K) higher. This will be discussed further in the next section.

Lean blow out (LBO) and ignition (IGN) tests were not part of the planned test program, yet observations made during startup and shutdown procedures were consistent with previous JP-8+100 testing. For a limited data set at a nominal 5% combustor pressure drop, LBO is nearly 40% of the (IGN) F/A for both 100% FT and JP8+100. The average LBO F/A values are

$$LBO_{100\%\,FT} = 0.0038 \pm 0.0004$$
$$LBO_{JP\text{-}8+100} = 0.0043 \pm 0.0004$$
$$(F/A)_{LBO\ 100\%\ FT}/(F/A)_{LBO\ JP\text{-}8+100} < 1$$

with some sensitivity to percent combustor pressure drop. The average ignition F/A values are

$$IGN_{FT} = 0.010 \pm 0.004$$
$$IGN_{JP\text{-}8+100} = 0.013 \pm 0.007$$
$$(F/A)_{IGN\ 100\%\ FT}/(F/A)_{IGN\ JP\text{-}8+100} < 1$$

No further tests were undertaken, and data at lower combustor pressure drops were insufficient to be definitive. Systematic altitude restart, ignition, and LBO studies are yet to be conducted.

Surface Thermal Measurements

The combustor walls and liners were instrumented for pressure and temperature. In general the pressure drop measurements are sensitive information and will not be presented as such. It should be noted that no inconsistent pressure measurements were found.

The liner and wall surface temperature locations are sensitive information and temperatures are noted as sidewall or liner (i.e., facing inside or outside).

For all figures herein, fuel compositions are denoted as follows: JP-8+100 is JP-8, Fischer-Tropsch is FT, and blended 50% JP-8+100 and 50% FT by volume is 50:50.

Sidewalls

Figure 3 illustrates that sidewall temperatures (TSW) strongly depend on F/A and weakly depend on fuel blend composition JP-8, FT, and 50:50. FWD represents forward; MID, middle; and AFT, the aft axial position of the thermocouple.

Unwrapped Combustor Liner

Figures 4(a), (b), and (c) represent unwrapped liner surface temperatures for three F/A values (0.010, 0.015, and 0.020) and three fueling compositions (JP-8, FT, and 50:50). The twin peaks represent sidewall (largest) and maximum inner liner temperatures, respectively. Temperature differences baselined to JP-8+100 are provided in Appendix B. We use the term "unwrapped" to mean the normalized outside liner surface circumference (0 to 1) to normalized inner liner circumferential surface (1 to 2) as a "continuous loop."

Figure 4(a) illustrates the unwrapped liner temperatures for F/A = 0.010 with outer liner temperatures to the left of the peak and inner liner temperatures to the right of the peak. The temperatures are slightly higher for the FT fueling.

Figure 4(b) represents unwrapped liner temperatures for F/A = 0.015 with outer liner temperatures to the left of the peak and inner liner temperatures to the right of the peak. The temperatures are lower for the FT fueling.

Figure 4(c) represents the unwrapped liner temperatures for F/A = 0.020 (JP-8) and 0.019 (FT) with outer liner temperatures to the left of the peak and inner liner temperatures to the right of the peak. The temperatures are lower for the FT fueling.

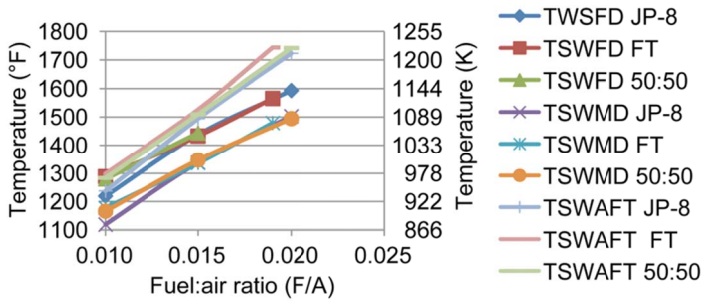

Figure 3.—Sidewall temperature variation with F/A and fuel composition.

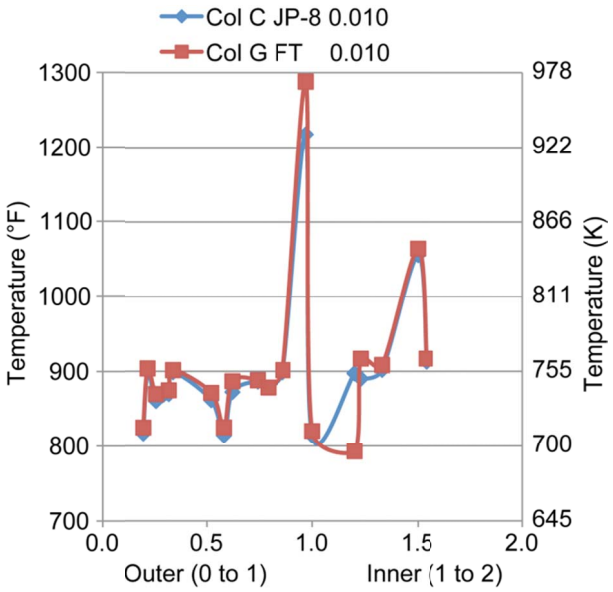

Figure 4(a).—Unwrapped liner temperatures for F/A = 0.010 and fueling compositions JP-8 and FT. Normalized combustor liner thermocouple locations: 0 to 1 outer and 1 to 2 inner.

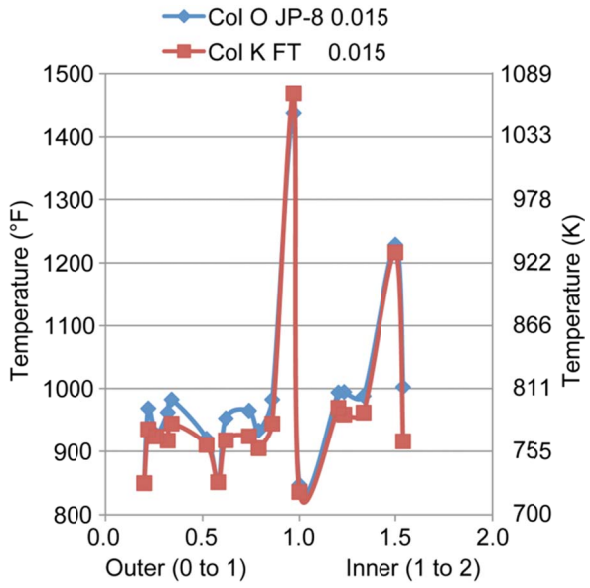

Figure 4(b).—Unwrapped liner temperatures for F/A = 0.015 and fueling compositions JP-8 and FT. Normalized combustor liner thermocouple locations: 0 to 1 outer and 1 to 2 inner.

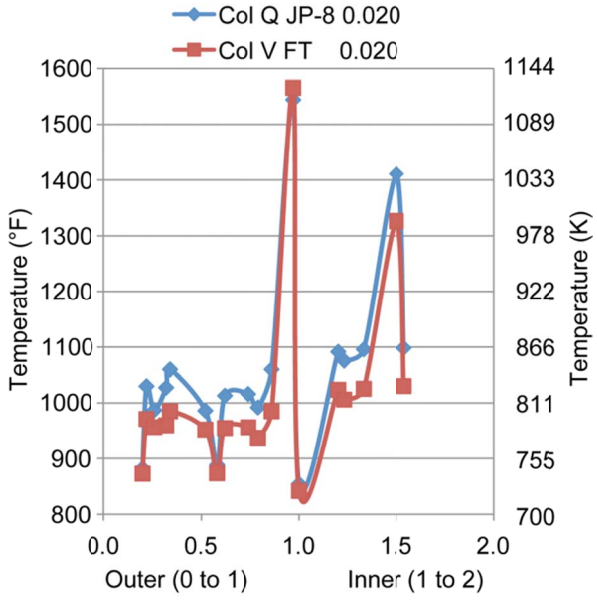

Figure 4(c).—Unwrapped liner temperatures for F/A ~0.020 and fueling compositions JP-8 and FT. Normalized combustor liner thermocouple locations: 0 to 1 outer and 1 to 2 inner.

Figures 5(a), (b), and (c) represent unwrapped liner surface temperatures differences relative to JP-8+100 as baseline, for three F/A values (0.010, 0.015, and 0.020) and three fueling compositions (JP-8, FT, and 50:50).

Figure 5(a) represents the unwrapped liner differences [$T_{fuel\ blend} - T_{JP-8}$] for F/A = 0.010 and fueling compositions 50:50 and FT. Normalized combustor liner thermocouple locations: 0 to 1 outer and 1 to 2 inner. JP-8 difference is 0. On average, the unwrapped liner temperatures are nominally 10 °F (6 °C) higher for FT and blended fueling than for JP-8 fueling, with actual differences given in Appendix B.

Figure 5(b) represents the unwrapped liner differences [$T_{fuel\ blend} - T_{JP-8}$] for F/A = 0.015 and fueling compositions JP-8 and FT. Normalized combustor liner thermocouple locations: 0 to 1 outer and 1 to 2 inner. JP-8 difference is 0. On average, compared with JP-8+100 fueling, the unwrapped liner temperatures are nominally 20 °F (11 °C) lower for FT fueling and 14 °F (8 °C) lower for 50:50 blended fueling; actual differences are given in Appendix B.

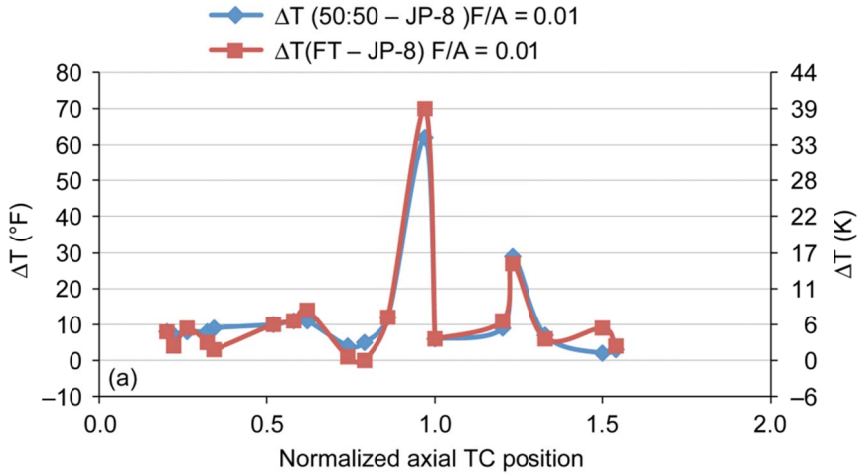

Figure 5(a).—Unwrapped liner temperature differences ΔT ($T_{fuel\ blend} - T_{JP-8}$) for F/A = 0.010 and fueling compositions 50:50 and FT. Normalized combustor liner thermocouple locations: 0 to 1 outer and 1 to 2 inner. JP-8 difference is 0.

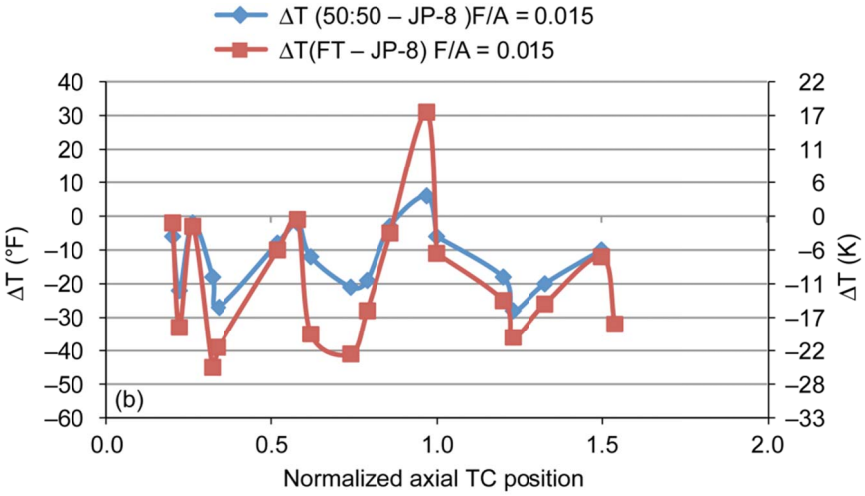

Figure 5(b).—Unwrapped liner temperature differences ΔT ($T_{fuel\ blend} - T_{JP-8}$) for F/A = 0.015 and fueling compositions JP-8 and FT. Normalized combustor liner thermocouple locations: 0 to 1 outer and 1 to 2 inner. JP-8 difference is 0.

Figure 5(c) represents the unwrapped liner temperatures differences [$T_{fuel\ blend} - T_{JP\text{-}8}$] (°F) for F/A ~0.020 and fueling compositions 50:50 and FT. Normalized combustor liner thermocouple locations: 0 to 1 outer and 1 to 2 inner. JP-8 difference is 0. On average, compared with JP-8+100 fueling, the unwrapped liner temperatures are nominally 45 °F (25 °C) lower for FT fueling and 18° F (10 °C) lower for blended fueling; see differences given in Appendix B.

Figure 6 shows that peak inner liner temperatures are nearly independent of fueling composition from 100% JP-8 to 100% FT.

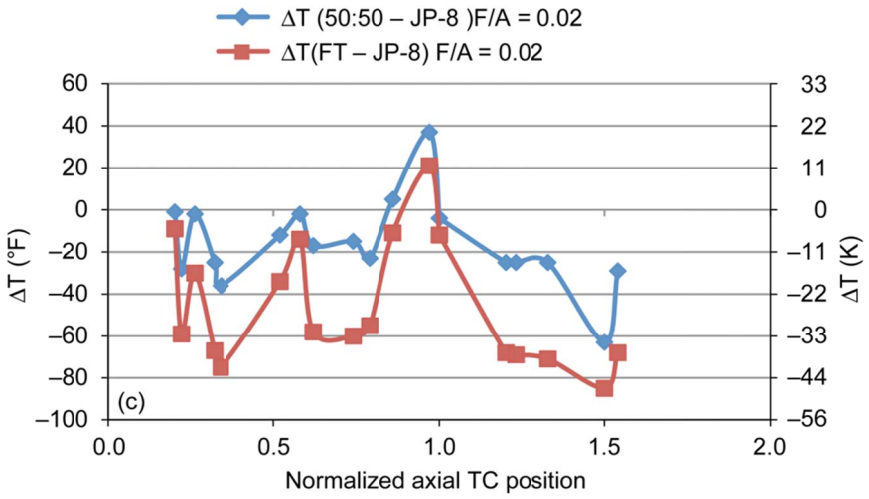

Figure 5(c).—Unwrapped liner temperature differences ΔT ($T_{fuel\ blend} - T_{JP\text{-}8}$) for F/A ~0.020 and fueling compositions 50:50 and FT. Normalized combustor liner thermocouple locations: 0 to 1 outer and 1 to 2 inner. JP-8 difference is 0.

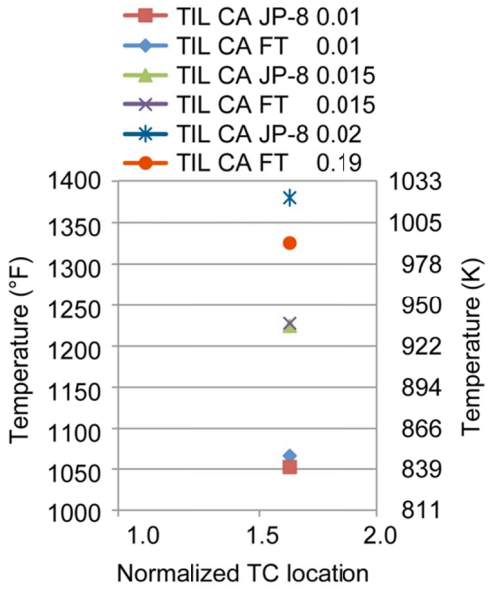

Figure 6.—Peak inner liner temperatures (TIL) at normalized location 1.5.

Combustor Inner and Outer Liner

Eliminating the sidewall peak temperature allows visualization of the smaller changes in surface temperatures. Omitting the peak temperature, Figures 7(a) through 7(f) illustrate major portions of the combustor liner axial and circumferential surface temperature variations with F/A and fueling composition. Throughout, the individual data points are connected by continuous curves for ease of comparison, not to imply the authors know or understand the physical processes occurring between data points.

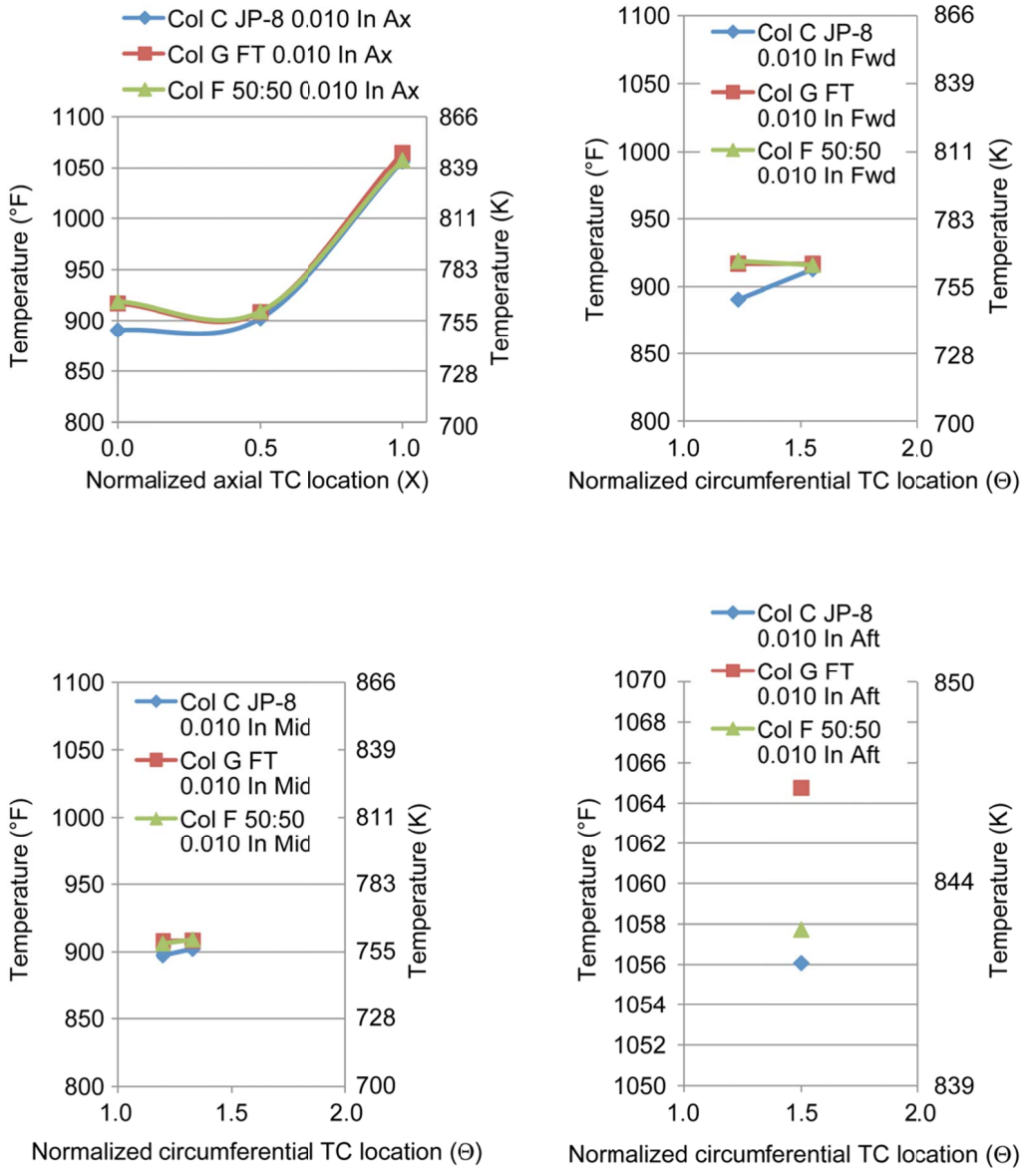

Figure 7(a).—Combustor liner inner surface temperature variations with fueling composition at F/A = 0.010.

Figures 7(a) and (b) illustrate variations of combustor axial and circumferential surface temperatures with temperature differences baselined to JP-8+100 in Appendix B, with distribution illustrated in Figures 5(a), (b), and (c). Figure 7(a) shows inner liner temperatures at F/A = 0.010 for fueling composition changes from JP-8 to FT. The temperatures for FT and blended fueling are slightly higher than for JP-8 fueling. Figure 7(b) shows variations of outer liner combustions temperatures at F/A = 0.010 for fueling composition changes from JP-8 to FT. The temperatures for FT and blended fueling are slightly higher than for JP-8 fueling.

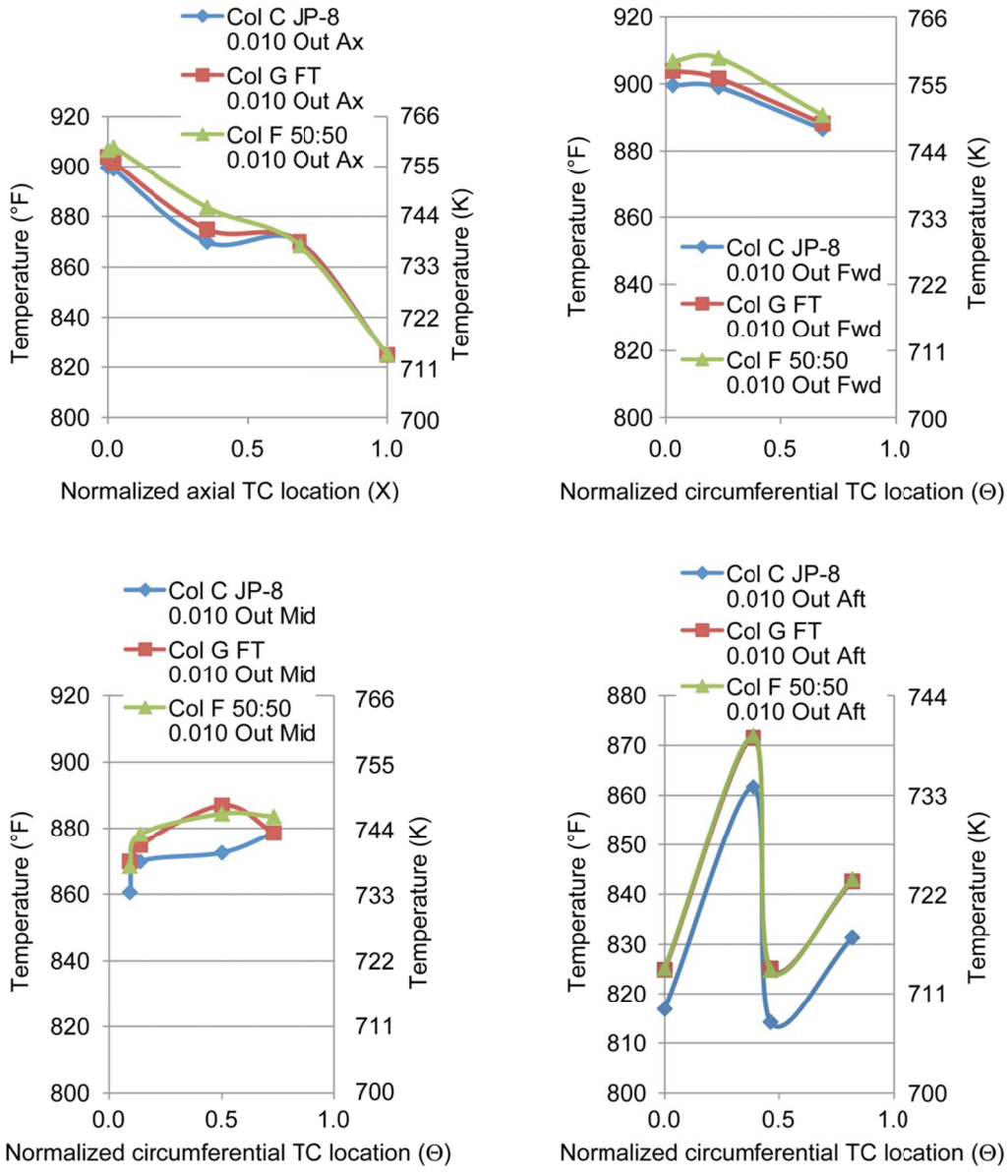

Figure 7(b).—Combustor liner outer surface temperature variations with fueling composition at F/A = 0.010.

Figure 7(c) shows variations of combustor outer liner temperatures at F/A = 0.015 for fueling composition changes from JP-8 to FT. Figure 7(d) illustrates variations of combustor inner liner temperatures at F/A = 0.015 for fueling composition changes from JP-8 to FT.

Figure 7(e) shows variations of combustor inner liner temperatures at F/A ~0.020 for fueling composition changes from JP-8 to FT. Figure 7(f) shows variations of combustor outer liner temperatures at F/A ~0.020 for fueling composition changes from JP-8 to FT.

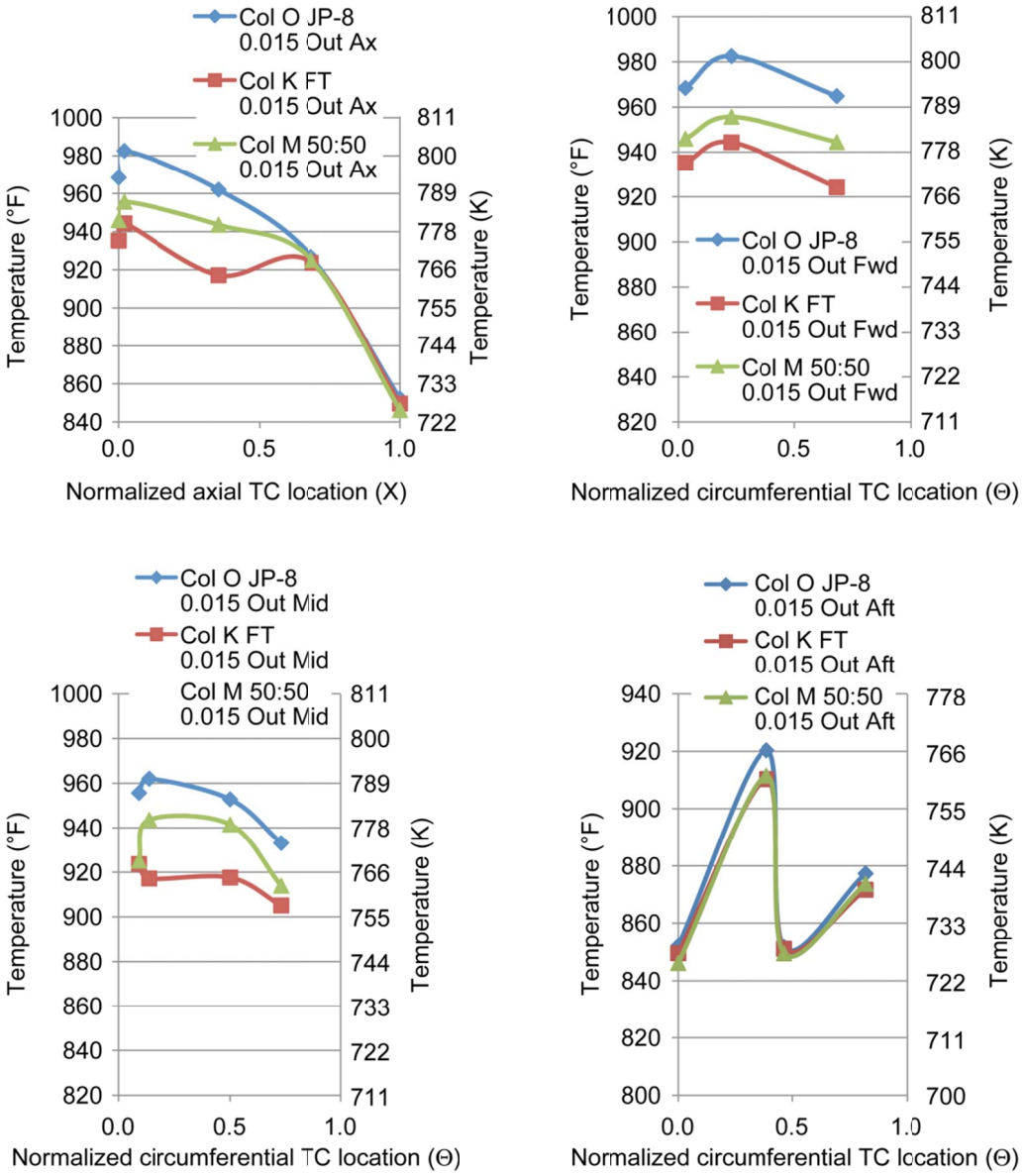

Figure 7(c).—Combustor outer liner temperature variations with fueling composition at F/A = 0.015.

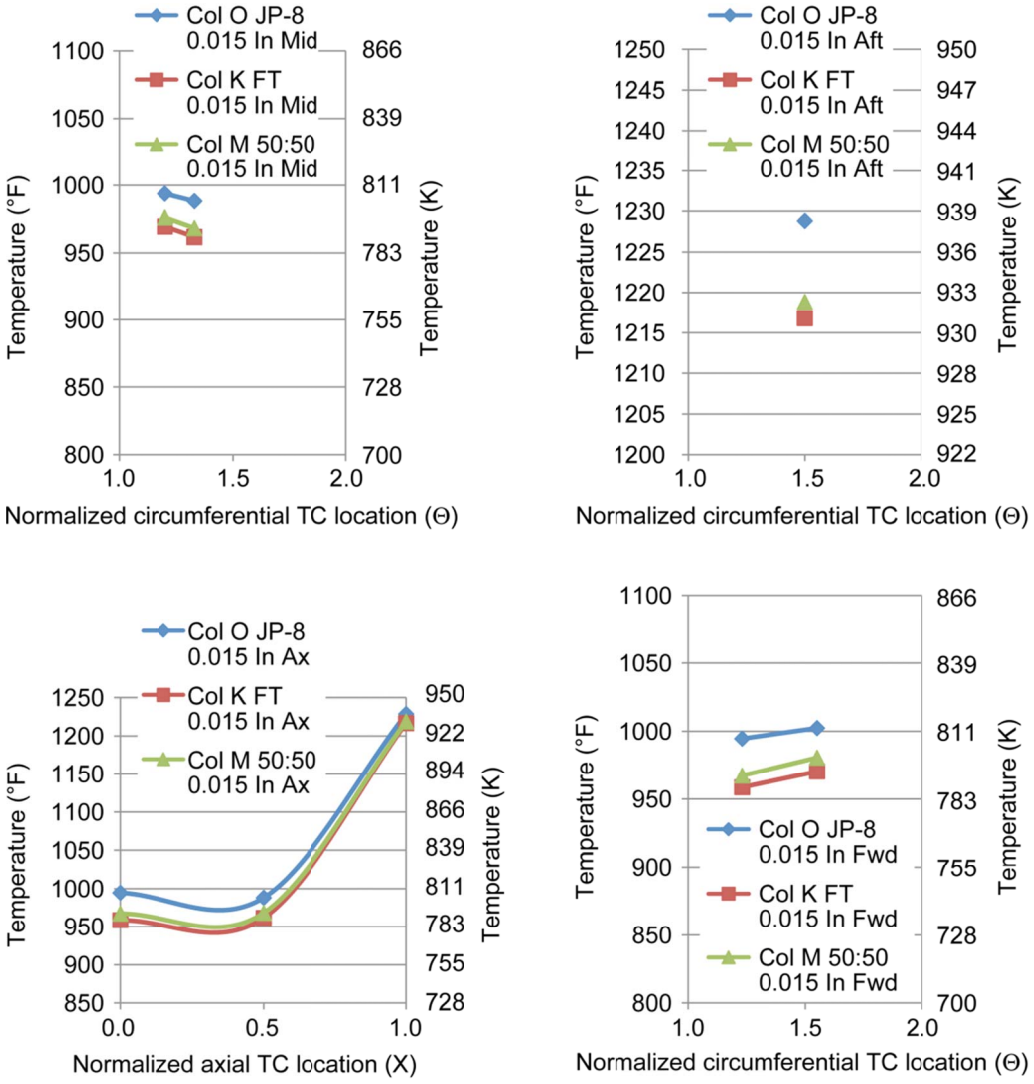

Figure 7(d).—Combustor inner liner temperature variations with fueling composition at F/A = 0.015.

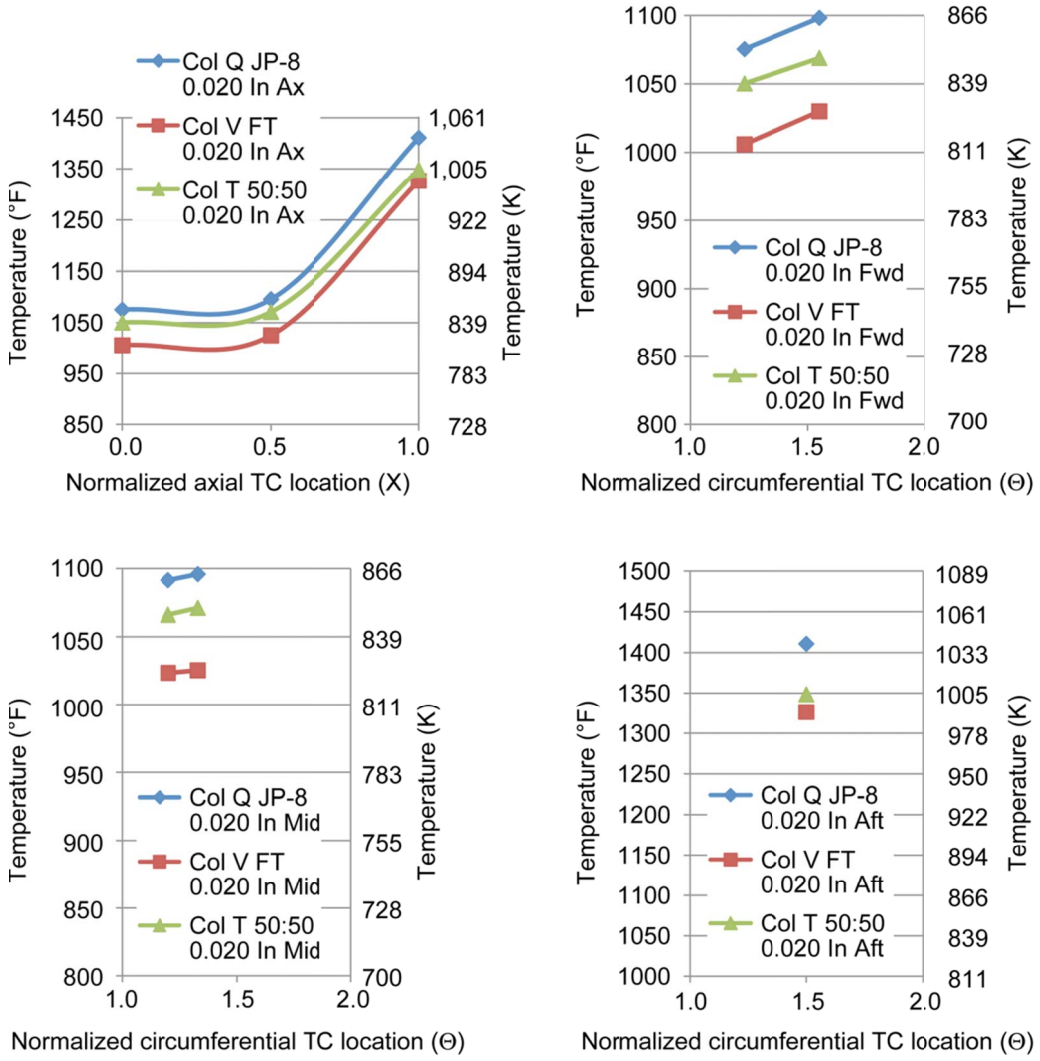

Figure 7(e).—Combustor inner liner temperature variations with fueling composition at F/A ~0.020.

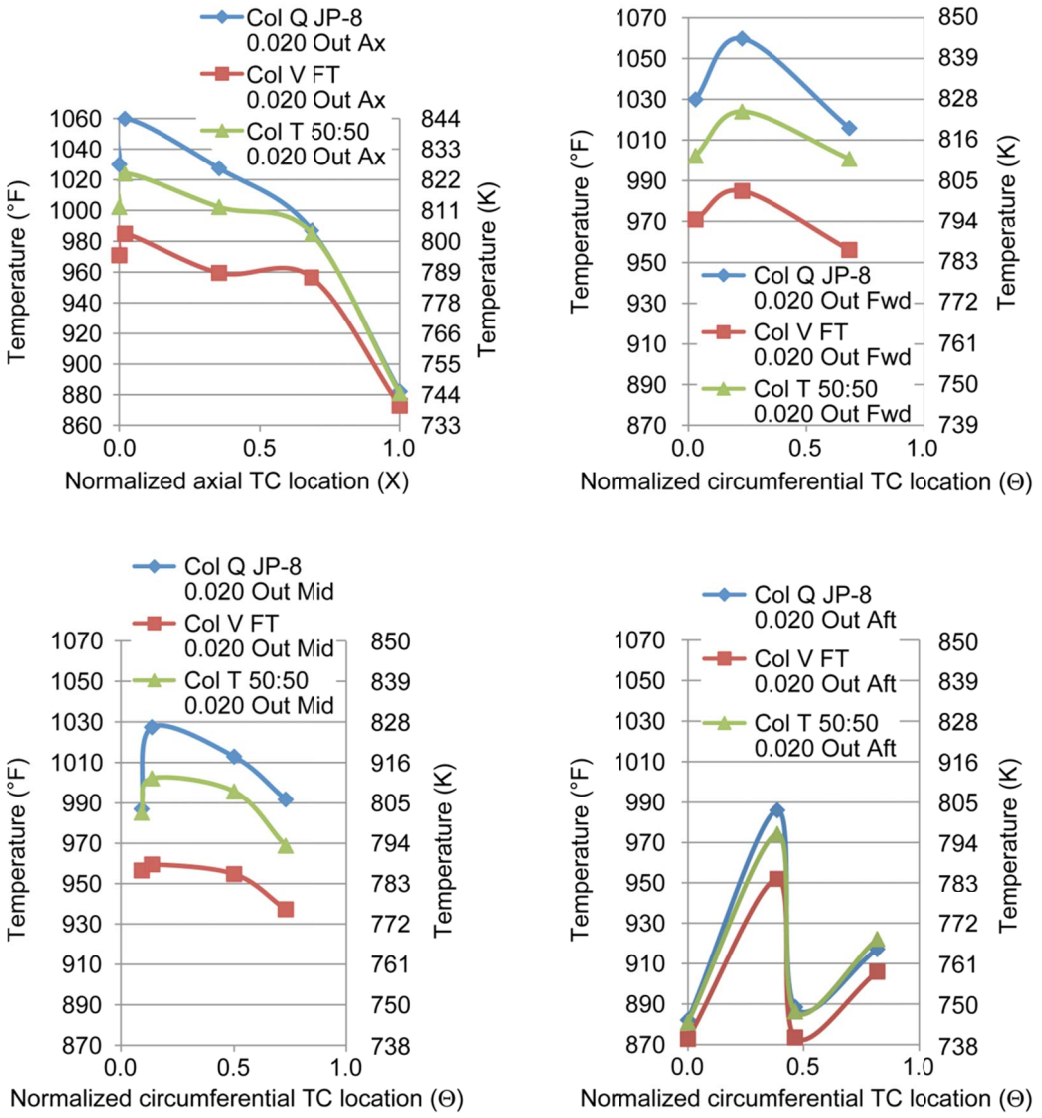

Figure 7(f).—Combustor outer liner temperature variations with fueling composition at F/A ~0.020.

Combustion Exhaust Rake Temperature

In the combustor thermal performance section, we noted that the SPK-FT calculated temperature based on emissions was higher than that of JP8+100 (Fig. 2). We now look at measured temperatures in the exhaust plane.

Three type-B metal thermocouples formed a thermal rake, [top (T), midplane (M), bottom (B)] to monitor the combustor exhaust. The top thermocouple was damaged by the exhaust plume after an initial set of test runs, restricting interpretation of exit plane temperatures, yet enough data were gathered prior to its loss to corroborate trends based on solely on the average of M and B readings. The exhaust plume was hotter at the top than the bottom which affects the turbine inlet pattern factor. Herein, temperature (T) > temperature (M) > temperature (B) with consistent trends for percent fueling as function of F/A, Figure 8. While dangerous to draw hard conclusions from sparse data sets, the trends are instructive. The linear locus fit to the SPK-FT and JP8+100 data show the SPK-FT exhaust temperature to be significantly higher than for JP8+100. With nearly equivalent slopes, the intercepts differ close to 88 °F (49 °C), which is higher but in reasonable agreement with the calculated flame temperature (Fig. 2), based on emissions. The significance is twofold: (1) higher turbine inlet temperatures provide higher engine efficiencies, and (2) component life decreases. Pattern factors are very important to turbine efficiency and component life can vary as much as 25% with a 10 °C change in temperature. The third dangerous part of having sparse data is making assumptions about the trending. Figure 9 shows the both the FT and 50:50 loci to be convex, whereas the JP8+100 locus is concave with a potential optimum near F/A = 0.015, implying cross-over points. Drawing implications outside the $0.01 \leq F/A < 0.02$ data set is not only unwarranted but dangerous.

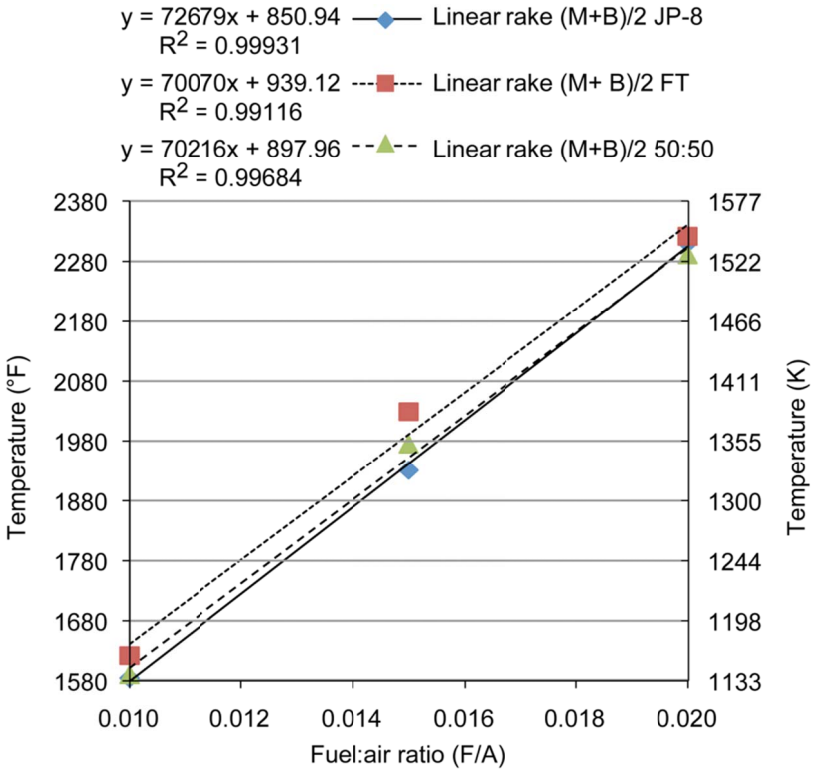

Figure 8.—Variation of exhaust plume temperatures with percent fueling as a function of fuel:air ratio (F/A).

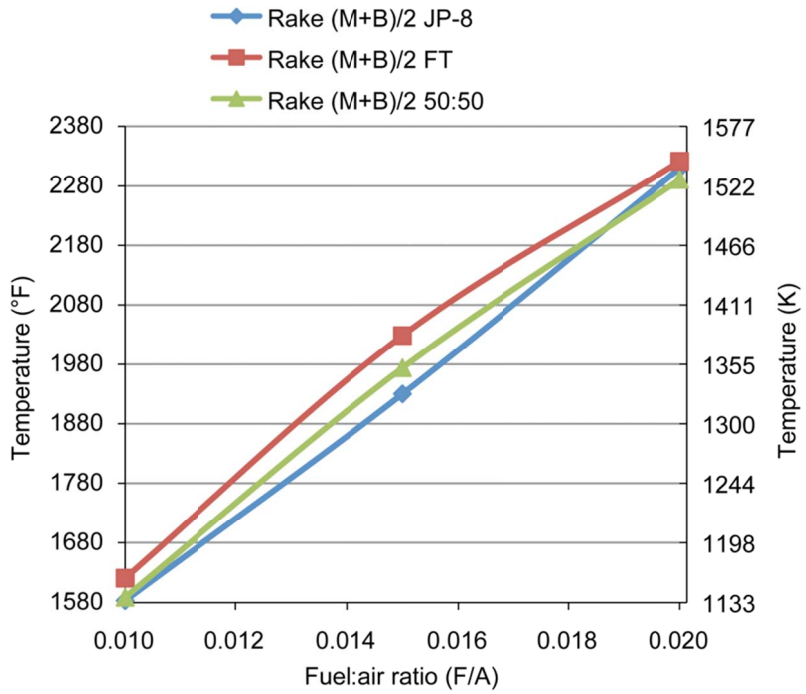

Figure 9.—Curvature of exhaust plume temperature loci with percent fueling as a function of fuel:air ratio (F/A).

Combustion Visualization

Digital camera exposures and high-speed photographs of the combustion process provide some insights for computational fluid dynamics (CFD) analysts (Ref. 3) as well as heuristic information for combustor designers: for example, luminosity variation with FT versus JP-8 concentration as illustrated in Figure 10(a), the digital camera pictures for F/A = 0.020. The general trend is increased luminosity with increased percent JP-8+100 and F/A.

High-speed video at 20 kfps illustrates the nature of the unsteady combustion processes (Figure 10(b) shows sequences from that video). The upper frames relate to JP-8+100 fueling (0% FT), and the lower frames relate to 100% FT fueling at two different fuel:air ratios (F/A). Both emissions and exit-plane thermocouple rake measurements indicate that FT fuels have higher heating values than JP-8+100, producing higher calculated and measured flame temperatures at the combustor exit, yet with lower liner temperatures. These observations are backed up qualitatively by observation of flame luminosity using a photo diode as well as pictures and high-speed video movies providing visual observations.

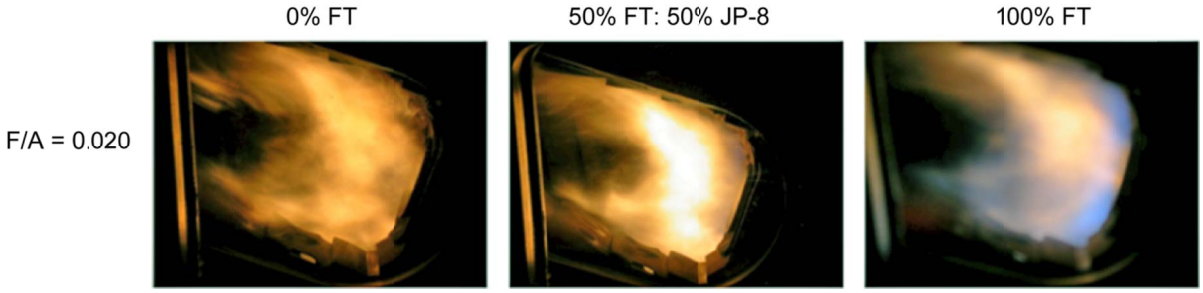

(a) Digital camera photographs illustrating changes in flame structure with changes in fuel blend at F/A= 0.020.

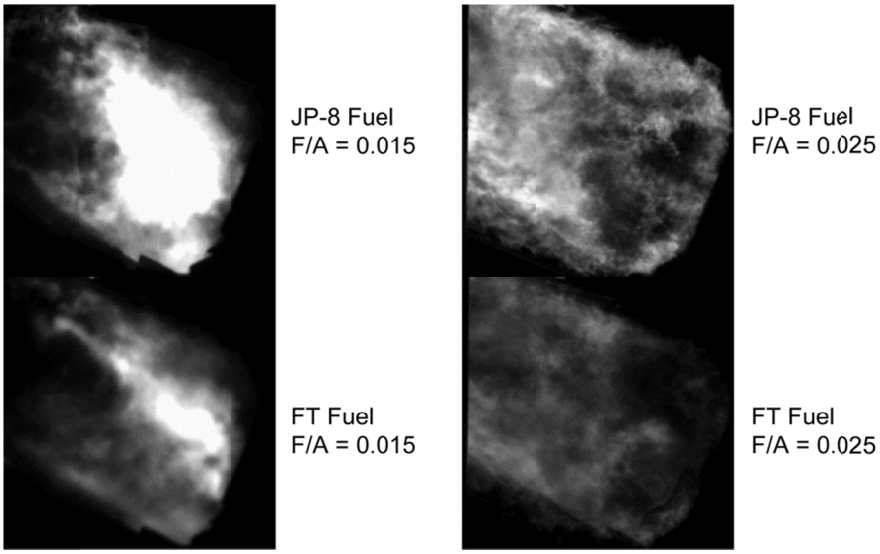

(b) High-speed video sequences comparing JP-8+100 fueling to FT fueling combustion at two different fuel:air ratios (F/A).

Figure 10.—Combustor A experiment photographs illustrating changes in flame structure with changes in fuel blend.

Conclusions: Part A

Alternate fueling testing is being carried out to determine preliminary performance, emissions, and particulates combustor sector data for SPK-type (e.g., Fischer-Tropsch) fuel blends, relative to JP-8+100 as baseline fueling, and to make projections for testing of biofuel fuel blends leading to preliminary development of smart fueling (fuel flexible) and combustor systems for the next generation aeronautic and aeronautic-derivative gas turbine engines. Herein alternate fueling test results for a well-characterized but proprietary combustor are provided for JP-8+100 and a Fischer-Tropsch- (FT-) derived fuel and a blend of 50% each by volume.

The test data presented are part of a more extensive data set where combustion parameters were varied over a range of values. The data herein are for the case of nominal inlet conditions at 225 psia and 800 °F (1.551 MPa and 700 K), and JP-8+100 is taken as baseline. These data provide the following results:

1. Combustor performance efficiencies at 0% FT (JP-8), at 50% blended FT and JP-8, and at 100% FT are nearly identical at about 99.9%.
2. Both outer and inner wall temperatures, on average, run
   a. warmer at F/A = 0.010 by 10 °F (6 °C) with FT fueling
   b. cooler at F/A = 0.015 by 20 °F (11 °C) with FT fueling
   c. cooler at F/A = 0.02 (0.019) by 45 °F (25 °C) with FT fueling

3. Sidewall temperature TSWFD ranges are 5.6% , 2.1%, and 1.4% higher for FT fueling for F/A = 0.01, 0.015, and 0.02, respectively. This may relate to the flame front moving away from the fuel injection interface.
4. Rake temperatures show core flow generally higher with FT than with JP-8, but one rake thermocouple (TC) was lost during testing, which inhibits conclusiveness.
5. All temperatures increase with F/A.
6. The 50:50 blend test results generally are between JP-8 and FT and somewhat closer to FT.
7. Lean blow out (LBO) and ignition (IGN) tests were not part of the planned test program, yet observations made during startup and shutdown procedures were consistent with previous JP-8+100 testing. For a limited data set at a nominal 5% combustor pressure drop, the F/A for LBO is nearly 40% of the IGN F/A for both 100% FT and JP-8+100. On the average, $(F/A)_{LBO\ 100\%\ FT}/(F/A)_{LBO\ JP\text{-}8+100} < 1$, with some sensitivity to percent combustor pressure drop, and $(F/A)_{IGN\ 100\%\ FT}/(F/A)_{IGN\ JP\text{-}8+100} < 1$. Definitive values at lower percent combustor pressure drops are insufficient for conclusions.
8. Altitude relight, ignition and LBO testing programs remain to be carried out.
9. High-speed photographs of the combustion process provide some insights for CFD analysts as well as heuristic information for combustor designers. For example, there was decreased luminosity with FT versus JP-8, and clips show enhanced vorticity for the conditions cited in Table 1.

Part B: Combustor Emissions

Part B presents gaseous emissions as CO_2, CO, and NOx (which also includes smoke and luminosity data); particulate emissions including distribution; and a brief comparison to small and large engine testing results from other programs. The emissions data are taken for the same tests and test conditions cited in Part A, nominally 225 psia at 800 °F (1.551 MPa at 700 K) with the sampling probe located at the nozzle exit plane. Emissions have a direct impact on aviation climatic constraints based on life cycle analysis (LCA) of fueling feedstocks, which includes fueling development and engine emissions. Herein the testing is directed toward fuel flex engine combustors, providing basic data for LCA fueling evaluations, where combustor A is one of several to be evaluated in development of fuel-flexible engine combustors.

Gaseous Emissions

Measurements for NOx were determined from combining NO and NO_2 measurements (Figs. 11(a) and (b). Nitric oxide (NO) with molecular atomic dimension (0.115 nm) (NO), while less than JP-8 at F/A = 0.010, steadily increases to become marginally higher than JP-8 at F/A = 0.020 (extrapolated) (Fig. 11(a)). Nitrogen dioxide (NO_2) (0.221 nm) (ppm) for FT or 50:50 blended fueling is considerably higher than for JP-8 and generally increases with F/A. Combining nitrogen dioxide (ppm) and nitric oxide (ppm), the trend with F/A and fuel composition is similar to that seen for NO; a slight decrease in NO_2: less than JP-8 at F/A = 0.010 and marginally higher than JP-8 at F/A = 0.020 (Fig. 11(c)).

Regarding the variation of $\%CO_2$ (0.0116 nm), ppm CO, and $\%O_2$, (Figs.12, 13, and 14, respectively), whereas each is strongly dependent with increasing F/A, the increase in $\%CO_2$ and ppm CO and the decrease in $\%O_2$ are marginally consistent with varied dependencies on fuel composition. The $\%CO_2$ appears somewhat consistent with decreased %CO and O_2 with fueling changes from JP-8 to FT, in agreement with flame temperature (Fig. 2).

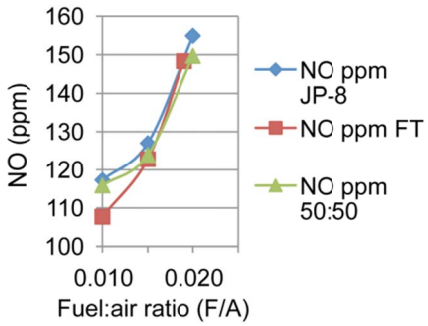

Figure 11(a).—Nitric oxide emission (ppm) variations with F/A and fueling composition.

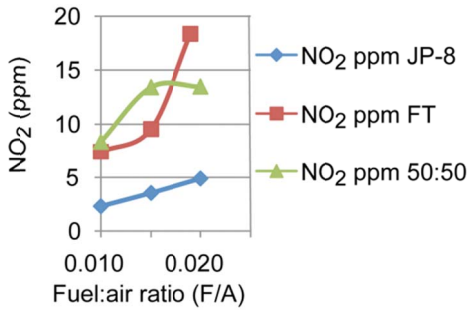

Figure 11(b).—Nitrogen dioxide emission (ppm) variations with F/A and fueling composition.

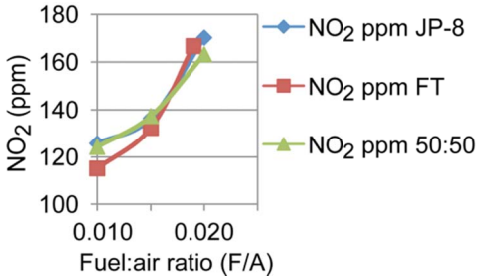

Figure 11(c).—NOx emission variations (ppm) with F/A and fueling composition.

[(g/kg) [EINOx or KHNOx] ≈ (ppm NOx) (1 + FAR)/(630 FAR)]. FAR = fuel:air ratio F/A [2]
[(g/kg) [EINOx or KHNOx] ≈ (ppm NOx) (1 + FAR)/(715 FAR)]. FAR = fuel:air ratio F/A (herein, arp)
[(g/kg) [EINOx or KHNOx] ≈ (ppm NOx) (1 + FAR)/(655 FAR)]. FAR = fuel:air ratio F/A (herein, arpc)
Aerospace recommended practice (arp) and (arpc) corrected arp

$EI_Z \approx [10^3 m_Z/m_f] \times [m_f (1+FAR^{-1})/m_{\text{gas products}}] \times [mol_Z M_Z/m_Z] \times [m_{\text{gas products}}/(\sum mol_j M_j)_{\text{gas products}}] \times 10^3/10^3 \times 10^{-6}$ ppm

m_X = mass flow rate of X (g/s), m_f = mass flow rate of fuel (kg/s), M_X = molar mass of X , mol_X = moles of X, and FAR = fuel:air ratio F/A

[(g/kg) [EINOx] SAE ARP 1533 ~ $(\{[NOx]/([CO]+[CO_2] + [C_xH_y]\} \times 10^3 M_{NOx}/(M_C + \alpha M_H)$

[NOx] [CO] [CO_2] [C_xH_y] = mass fractions of NOx, CO, CO_2, and total hydrocarbon THC, M = molar mass, α = ratio of H/C = n/m in fuel C_mH_n where NOx mol mass is assumed to be 46; contrast to Figures 11(a) and 11(b)

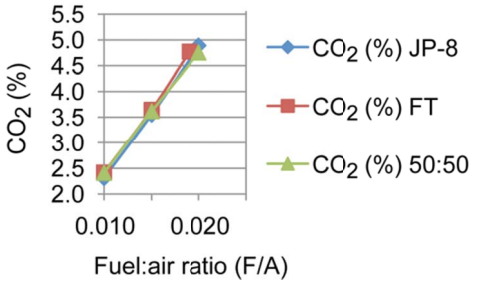

Figure 12.—Variation of %CO_2 with F/A and fuel composition.

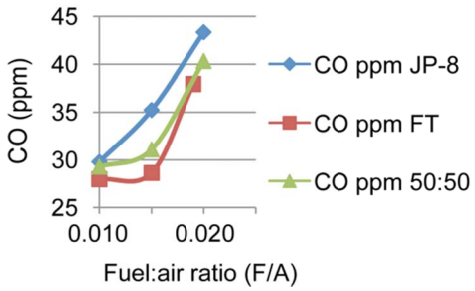

Figure 13.—Variation of CO (ppm) with F/A and fuel composition. [(g/kg) EICO ≈ (ppm CO) (1+ FAR)/(1220 FAR)]. FAR = fuel:air ratio F/A.

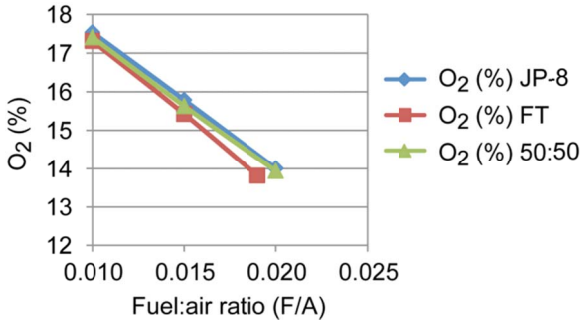

Figure 14.—Variation of $\%O_2$ with F/A and fuel composition.

Figure 12 shows the strong variation of $\%CO_2$ with F/A, but it is nearly independent of fuel composition. However, it appears somewhat consistent with decreased $\%O_2$ with fueling changes from JP-8 to FT. Carbon monoxide (0.113 nm) (CO) generally is lower with fueling from JP-8 to FT with some changes at F/A = 0.019, which extrapolated is unresolved (Fig.13). The decrease in $\%O_2$ (Fig. 14) is consistent with increasing F/A—as well as higher rake temperatures—with FT, indicating increased combustion temperatures with more complete combustion (Fig. 2).

Smoke and Photo Diode Numbers

The smoke number (SN) is dimensionless [(mg-C)/s / (kg-combustor gas)/s]. It is measured by drawing a sample of exhaust through a filter paper, then comparing the change in the reflectance between the "non-stained" and "stained" paper. Smoke number, NOx, CO, and HC measurements are all made in the exhaust plane. Representative averages are provided to certificating authorities at several engine operating conditions. The general trend of total hydrocarbon emissions (THC) (Fig. 15) strongly depends on fuel:air ratio F/A and is less dependent on fuel blend except with FT at F/A = 0.015. The reason is not known at this time, nor is it entirely clear that for all intents and purposes why THC is nearly independent of fuel composition because the smoke data do show more distinctive trends with fueling composition at F/A = 0.010 (Fig. 16). For FT fueling, the smoke number is well below that of JP-8 at F/A of 0.01 and 0.02, yet they are nearly the same at F/A = 0.015. FT smoke number increases with F/A, but it is not clear for either JP-8 or 50:50 blended fuel.

Smoke number and THC results reinforce the necessity for good particulate measurements, their distribution, composition, and toxicology.

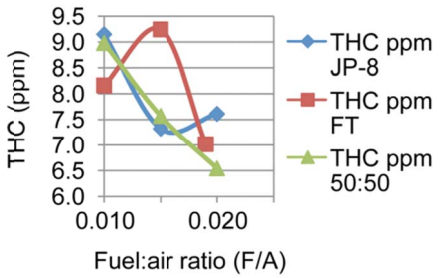

Figure 15.—Total hydrocarbon variations, THC (ppm) with F/A and fuel composition. [(g/kg) THC ≈ (ppm THC) (1+ FAR)/(2070 FAR)]. FAR = fuel:air ratio F/A.

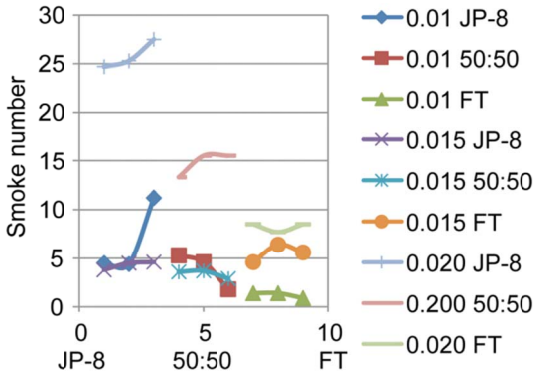

Figure 16.—Smoke number variations with F/A and fueling composition.

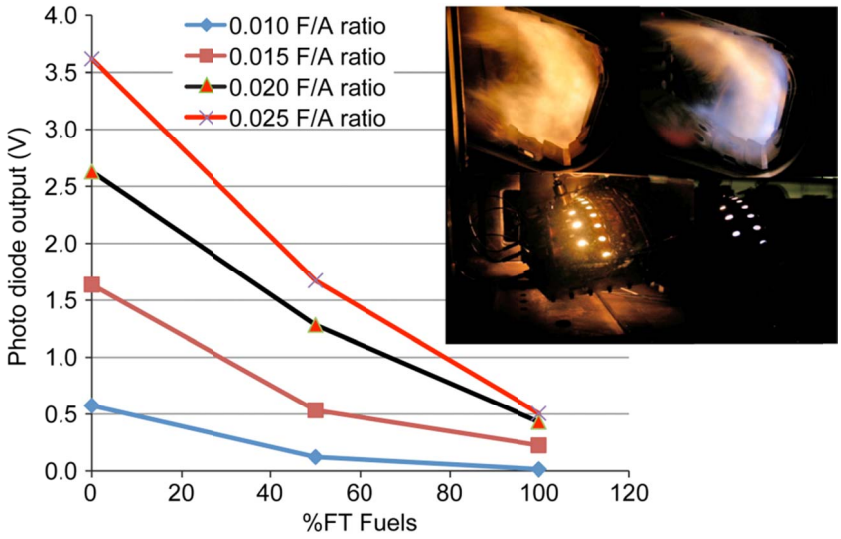

Figure 17.—Variation in photo diode voltage output with fuel blending at various F/A values for 100% JP-8 and 100% FT fueling as well as 50% blend of JP-8 and FT fuel; $(P,T)_{inlet}$ is [75 psia (0.517 MPa), 500 °F (533 K)] at 3% combustor pressure drop. Photo on left is 100% JP-8 and on the right 100% FT at F/A =0.010.

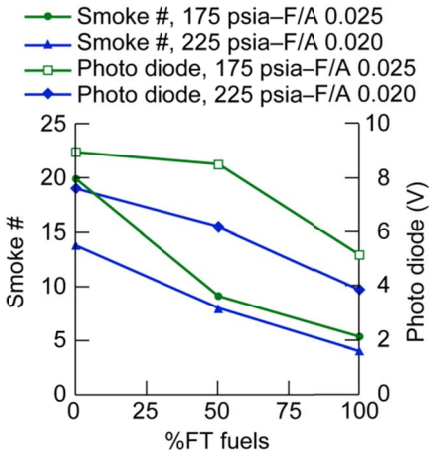

Figure 18.—Smoke number variations with %FT fueling for combustor inlet pressures of 175 and 225 psia (1.207 and 1.551 MPa) at F/A = 0.020 and 0.025. Results imply reductions in polycyclic aromatic hydrocarbons (PAH) (soot) and polycyclic aromatic compounds (PAC).

[Note: FT fuels have few if any aromatics and lower total particulates.]

Figure 17 illustrates the change in flame luminosity on a relative basis as the blend of JP-8 and FT fuel is varied. Optical access windows are combustor pressure limited, and the data set shown is at $(P,T)_{inlet}$ (75 psia (0.517 MPa), 500 °F (533 K)) at 3% combustor pressure drop.

The increase in flame luminosity follows the same trends for collected smoke data as shown in Figure 18. The decline in smoke number with increasing FT fueling is most pronounced at lower F/A values. Smoke number consistently increases with F/A independently of fueling yet is lowest at 100% FT fueling. A striking feature is the decrease in relative flame luminosity as illustrated in Figure 17 with the characteristic clean blue flame at 100% FT fueling. This increase in smoke number and flame luminosity as the fuel blend is increased to 100% JP-8 suggests that the radiation heat load on the combustor increases as well at higher F/A values; the wall metal temperatures corroborate this increase.

Figure 18 illustrates a decrease in smoke number as combustor pressure changes from 175 to 225 psia (1.207 to 1.551 MPa) (note the anomaly at 175 psia (1.207 MPa)) with consistent increases in smoke number and photo diode emissions with increased F/A from 0.020 to 0.025. In general these trends corroborate the particulate data shown later.

Particulate Emissions

The particulate distribution depends on engine power setting, pressure, F/A and fueling composition, and the chemical nature of the particulates and their toxicity. Such data are necessary for determination of environmental health hazards, cloud formations, and climatic changes.

To demonstrate the operability of the emissions probes, the test F/A values were compared with the CO_2-based F/A values. The 100% FT and 50:50 blends are within +12% to –18% of one-to-one correspondence whereas the 100% JP-8 is +8% to –34% with one point at –50%. The general trends are for FT and blends to be consistently higher and JP-8 lower than one-to-one correspondence (Fig. 19). Such evidence may reflect the paraffinic nature of FT and the high aromatic and cyclohydrocarbon content of JP-8.

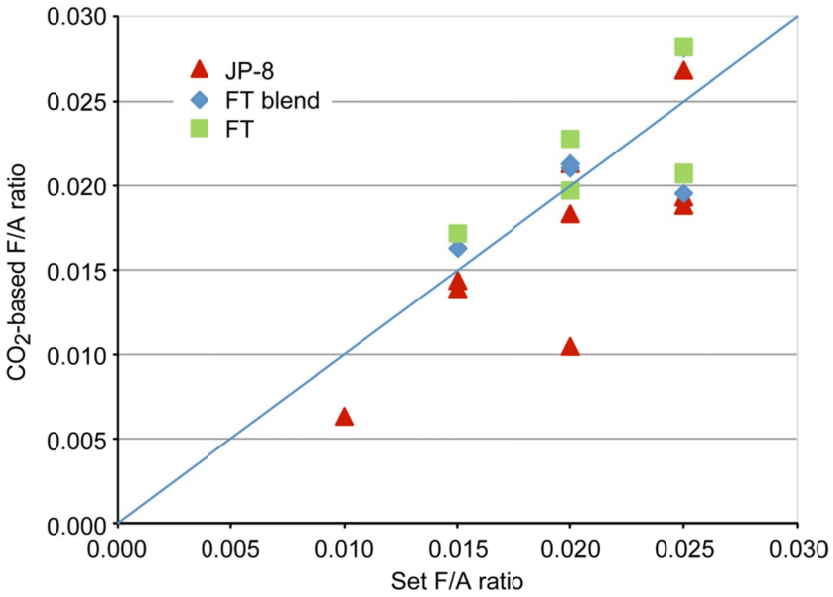

Figure 19.—Alternate fuel experimentally set F/A versus CO_2-based calculated F/A.

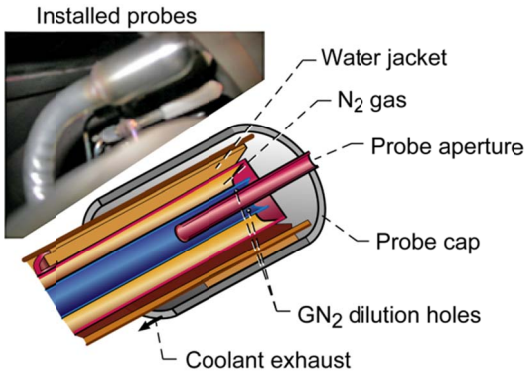

Figure 20.—Emissions probes installed at combustor exhaust exit plane. Particulate probe is in photo foreground with gas emissions/TC rake probes in background. Details of the water cooled, nitrogen gas dilution particulate probe shown in inset. Probe cap outer diameter = 0.075 in. (19 mm) with aperture diameter 0.044 in. (1.12 mm). Both diluted and undiluted probes were installed. Photo of installed probes shown rotated out of true combustor exhaust plane position.

The nitrogen gas tip-diluted, water-cooled particulate probe is illustrated in Figure 20. Because of in-plane hardware details, the photo and detail insert are shown rotated out of true exhaust plane. The probe cap outer diameter = 0.075 in. (19 mm) with aperture diameter 0.044 in. (1.12 mm). The probe aperture aspirated exhausted gas steam is quenched by water cooling, which also prevents probe failures from overheating. Both diluted and undiluted probes were positioned at the combustor exhaust plane. For the dilution probe, the exhaust gas is further cooled and diluted with nitrogen gas. Both types are held above condensation temperature of water and organics en route to the instrumentation sampling panel. Details of the facility and gas emissions sampling probes are given in Shouse et al. (Ref. 2).

In terms of particle emissions indices EI_n, the general trends with both pressure and F/A are higher EI_n values (number/kg-fuel burn) for JP-8 and lower values for FT with the 50% blend (50% JP-8 and 50% FT) in between (Fig. 21). At an F/A of 0.015, the FT emissions index EI_n –FT is nearly ¼ that of JP-8 at

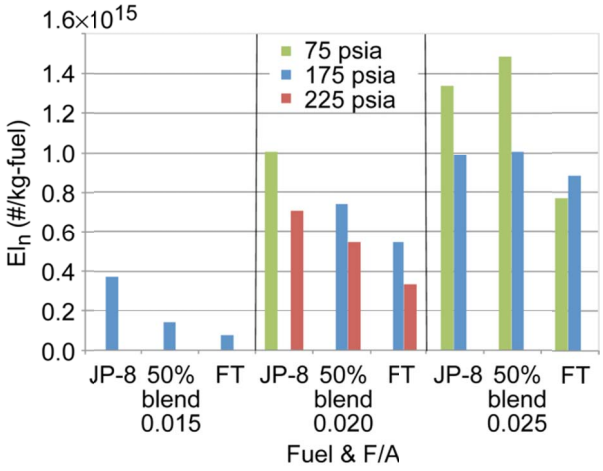

Figure 21.—Particulate emissions number indices variations with test pressure and F/A for JP-8, FT blend, and FT fueling. [Note: Test data set incomplete at 75 psia and 225 psia for FA = 0.015 and at 225 psia for FA = 0.025.]

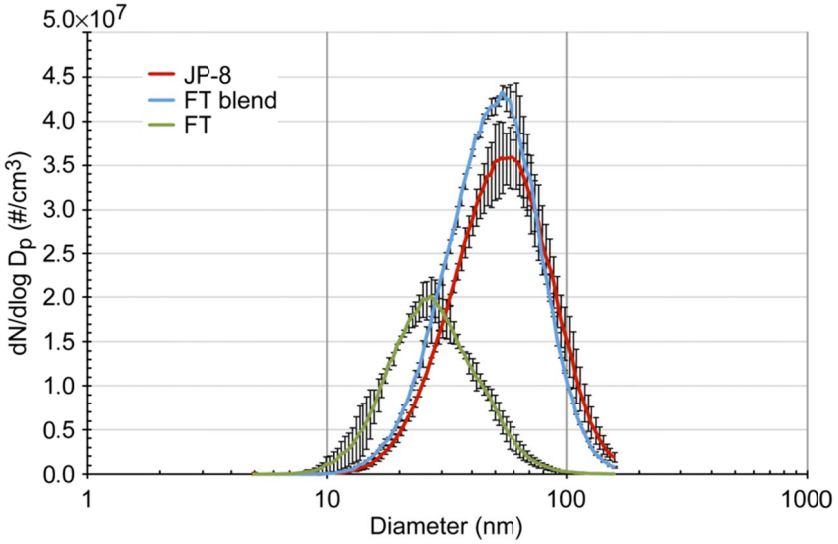

Figure 22.—Alternate fueling particle size distribution with JP-8, FT blend, and FT for combustor pressure at 75 psia (0.517 MPa) and F/A = 0.025. dEI/d(log Dp) = 2.833×10^3 [dN/d(log Dp)][(1+ FAR)/FAR](T/P) where N = number/cm^3, EI = number/kg, and FAR = fuel:air ratio F/A; P is instrument pressure in atmospheres and T is temperature in K (herein 1 atm and ~293 K).

175 psia (1.207 MPa); at F/A = 0.020, nearly ½ at 225 psia (1.551 MPa); and at F/A = 0.025, nearly 7/8 at 175 psia (1.207 MPa). Note, however, the variability of 50% fuel blend at lower pressures of 75 psia (0.517 MPa). Whereas it is difficult to make a direct comparison with on-wing engine testing, the data trends are consistent where FT particulate emissions are much lower than Jet A at low power (lower engine pressure), yet the difference trend diminishes with increased engine power (higher engine pressure).

Trends with the cleaner paraffinic fuels (FT) are also reflected in terms of particulate size distribution (Fig. 22) but not necessarily in terms of the FT blend, where at 75 psia (0.517 MPa) anomalous behavior is observed, namely the number of particulates (N) of size Dp (equivalent diameter) per cubic centimeter increases beyond that of JP-8. However for FT fueling, the values of the [dN/d(log D_p)] derivative

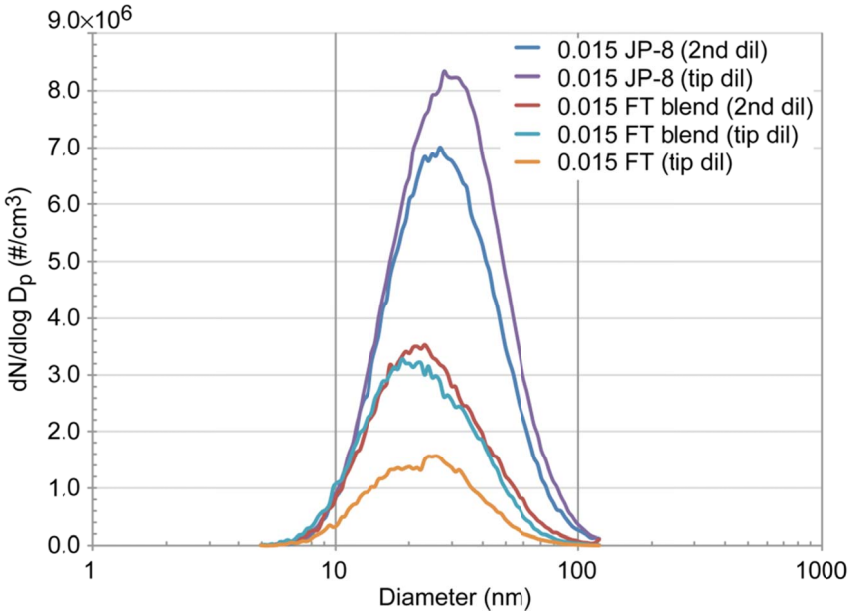

Figure 23.—Particulate size distribution changes with probe dilution with JP-8, FT blend, and FT fuels for combustor pressure 125 psia (0.862 MPa) and F/A = 0.015. $dEI/d(\log Dp) = 2.833\times10^{3}$ [dN/d(log Dp)][(1+ FAR)/FAR](T/P), where N = number/cm^3, EI = number/kg, and FAR = fuel:air ratio F/A; P is instrument pressure in atmospheres and T is temperature in K (herein 1 atm and ~293 K).

indicate the total particle counts (integrals) are nearly half that of JP-8. Note the peak shift toward smaller diameter particulates, and the smaller (about half the size of the JP-8 peak) particulates making more difficult to detect, isolate, collect and dispose of such particulates. Further, the toxicology requires much study.

Particulate size and to some extent, distribution, are highly dependent on the probe. Effects of probe tip dilution and probe secondary dilution are illustrated in Figure 23 for combustor pressure of 125 psia (0.862 MPa) and F/A = 0.015. Here the trend with particulate size is not as definite as illustrated in Figure 22, and the effects of probe dilution diminishes with fuel blending.

Looking again at the anomalous trends at combustor pressure of 75 psia (0.517 MPa) and 175 psia (1.207 MPa) shown in Figures 21 and 22, shows similar trends in particulate distribution (Fig. 24). Whereas the cleaner FT fuel particulate peak is still less than that of JP-8 or the FT blend, the trend is minor by comparison with those shown in Figure 21 at other pressures. While consistent, the behavioral reasons remain to be explored.

In contrast to the distribution trends at combustor pressure of 75 psia (0.517 MPa) and 175 psia (1.207 MPa) and F/A = 0.025 (Fig. 24), the trends at combustor pressure of 225 psia (1.551 MPa) and F/A = 0.020 are consistent with clean fuel blending; namely JP-8 produces more particulates than the FT blend and far more than FT fueling (Fig. 25). The variation with JP-8 fueling is also illustrated as JP-8(2) on the figure. Less pronounced is the variation in the particulate peaking which is more consistent with that of Figure 24.

The mean particle diameter at 175 psia (1.207 MPa) decreases with fueling blend from JP-8 to FT (Fig. 26). This trend is not evident in Figure 24, adding to the complexity of predicting combustor particulate variations.

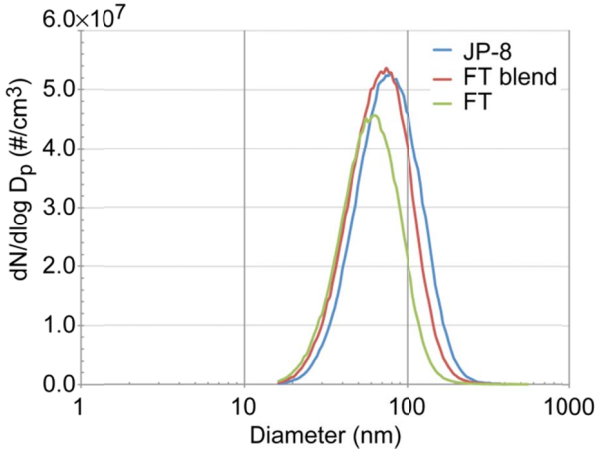

Figure 24.—Particle size distribution with JP-8, FT blend, and FT for combustor pressure 175 psia (1.207 MPa) and F/A = 0.025. dEI/d(log Dp) = 2.833×10^3 [dN/d(log Dp)][(1 + FAR)/FAR](T/P), where N = number/cm^3, EI = number/kg, and FAR = fuel:air ratio F/A; P is instrument pressure in atmospheres and T is temperature in K (herein 1 atm and ~293 K).

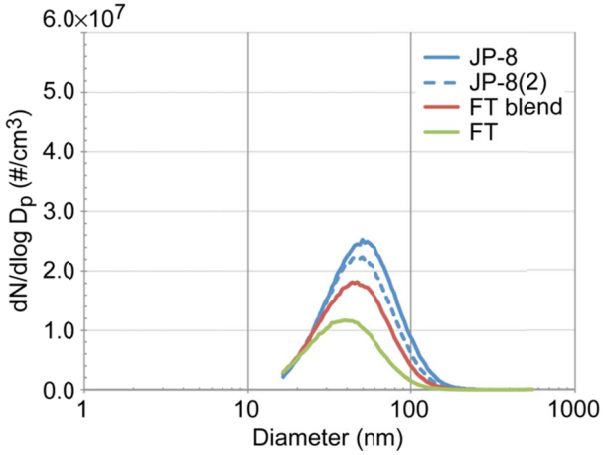

Figure 25.—Particulate size distribution for JP-8, FT blend, and FT fueling at combustor pressure 225 psia (1.551 MPa) and F/A = 0.020. dEI/d(log Dp) = 2.833×10^3 [dN/d(log Dp)][(1 + FAR)/FAR](T/P), where N = number/cm^3, EI = number/kg, and FAR = fuel:air ratio F/A; P is instrument pressure in atmospheres and T is temperature in K (herein 1 atm and ~293 K).

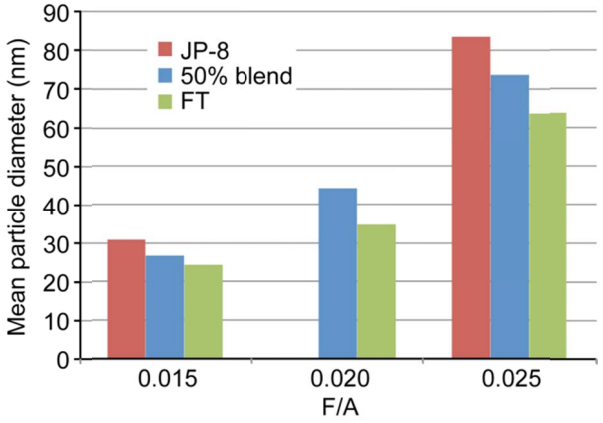

Figure 26.—Mean particle diameter with JP-8, FT blend, and FT fueling for combustor pressure 175 psia (1.207 MPa) and F/A values of 0.015, 0.020, and 0.025.

Engine Emissions Testing

Other emissions and peformance tests indicate small to no changes in emssions within limits as prescribed in the Jet A fueling specifications (Ref. 4).

A collaborative [NASA, AFRL, Arnold Engine Development Center (AEDC)/ATA, Aerodyne Research Inc. (ARI), Environmental Protective Agency (EPA), Missouri University for Science and Technology (MST), ASRC Aerospace Corp., Science Systems and Applications Inc. (SSA); University of Dayton Research Institute (UDRI), United Technoloigies Research Center (UTRC), Pratt-Whitney Aircraft (P&W),] and others small and large on-wing engine emissions and performance test program provides several needed insights into aviations emissions (Refs. 5 and 6).

Small Engine Testing

Small-engine test stand observations on a test-stand-mounted PW 308 engine fueled by JP-8, FT, and FT-blended fuels:

At low power,
- NOx emissions are within instrument measurement capabilities
- Lower CO emissions with FT/blend may be due to higher H/C ratio

At intermediate or high power,
- Very low CO emissions make ratios irrelevant to evaluate differences between the fuels
- There is no significant difference in NOx emissions

These tests also revealed negligible unburned hydrocarbons (UHC) at all power conditions for both of the two FT fuels tested. The SO_2 emissions indicate the sulfur content of the blend to be around 50% of that for JP-8, whereas for 100% FT fuel a value of 0.1% indicates contamination.

Approximately 2% fuel flow benefit with 100% synthetic fuel can be attributed to the higher heat content of synthetic fuel. Rahmes et al. (Ref. 7) provides emissions results for an unspecified fuel that was tested in a Pratt & Whitney small turbine engine (inferred as PW 308 and biofueling). Emissions deviations were small except for core smoke (Fig. 27). The particulate distributions change with both fueling (F/A) and engine power settings, showing decreases in emissions with increses in %FT and increases with engine power setting (Figs. 28 and 29). Figure 30 provides a comparison of mean particulate diameters for JP-8, 50:50 blend, and FT fueling with changes in engine power for the PW 308 off-wing engine testing.

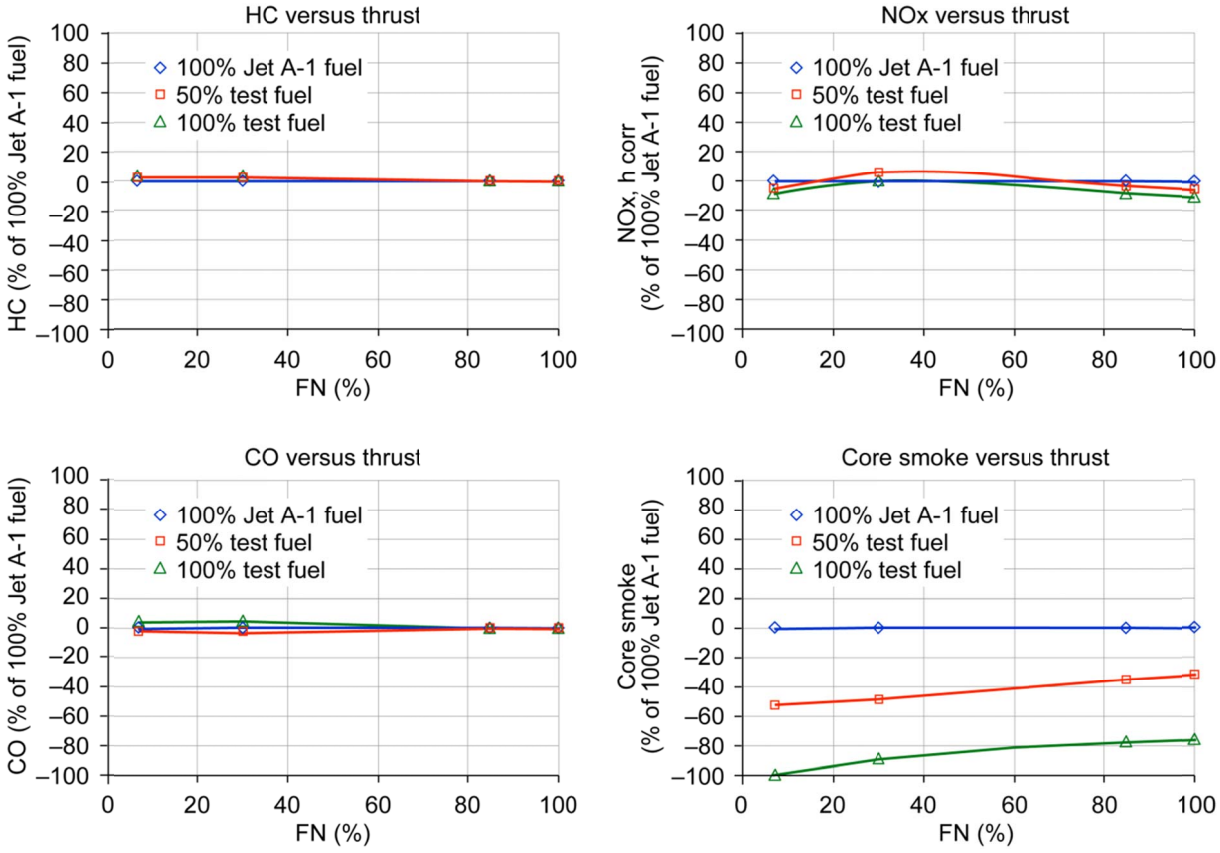

Figure 27.—Small turbine engine emissions test results (Ref. 7).

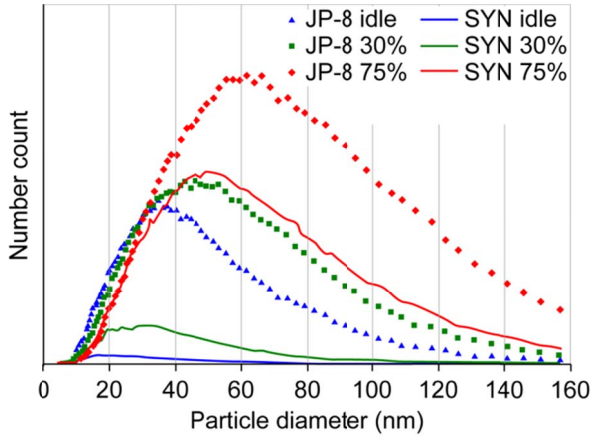

Figure 28.—Variation of particulate distribution with fueling changes (alternative fuels PW 308 engine testing).

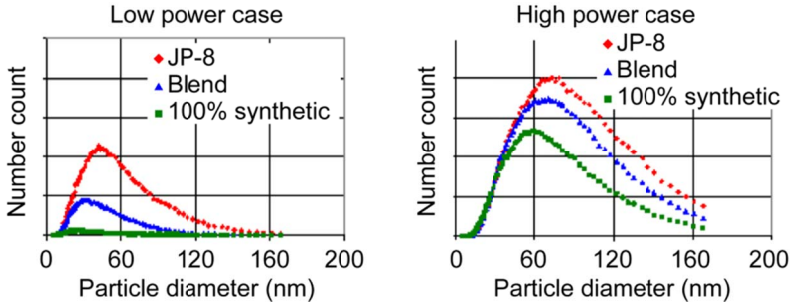

Figure 29.—Changes in particulate distribution with power and fueling (alternative fuels PW 308 engine testing).

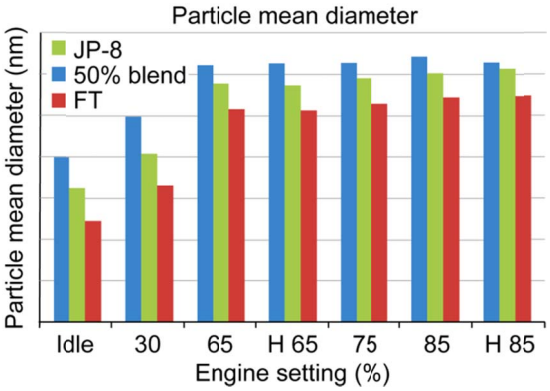

Figure 30.—Variations of mean particulate diameter with fueling and power level (alternative fuels PW 308 engine testing).

Large Engine On-Wing Test Results

A consortium of agencies are working together to provide on-wing engine emissions testing for 100% JP-8 or Jet A1 (JP-8 without military additives), a 50:50 blend with SPK, and 100% SPK engine fueling at various power settings. Here SPK represents different Fischer-Tropsch fuels depending on feedstock and refiner. Future testing will include biomass feedstock fueling (HRJ). For these tests the fuel was either coal- or gas-derived jet fuel. Particulate distributions given by Anderson (Ref. 8) at 30% and 65% engine power setting are provided on the left side of Figure 31. The number of particulates and black carbon values are provided on the right side of Figure 31.

The data presented herein show a strong dependence on F/A and blend with an implied less dependency on fuel composition. The small-engine test data figures are both normalized and too coarse to illustrate the dependencies for the data herein. As for the on-wing engine test results, the AAFEX program data are planned to be released in a January 2010 workshop.

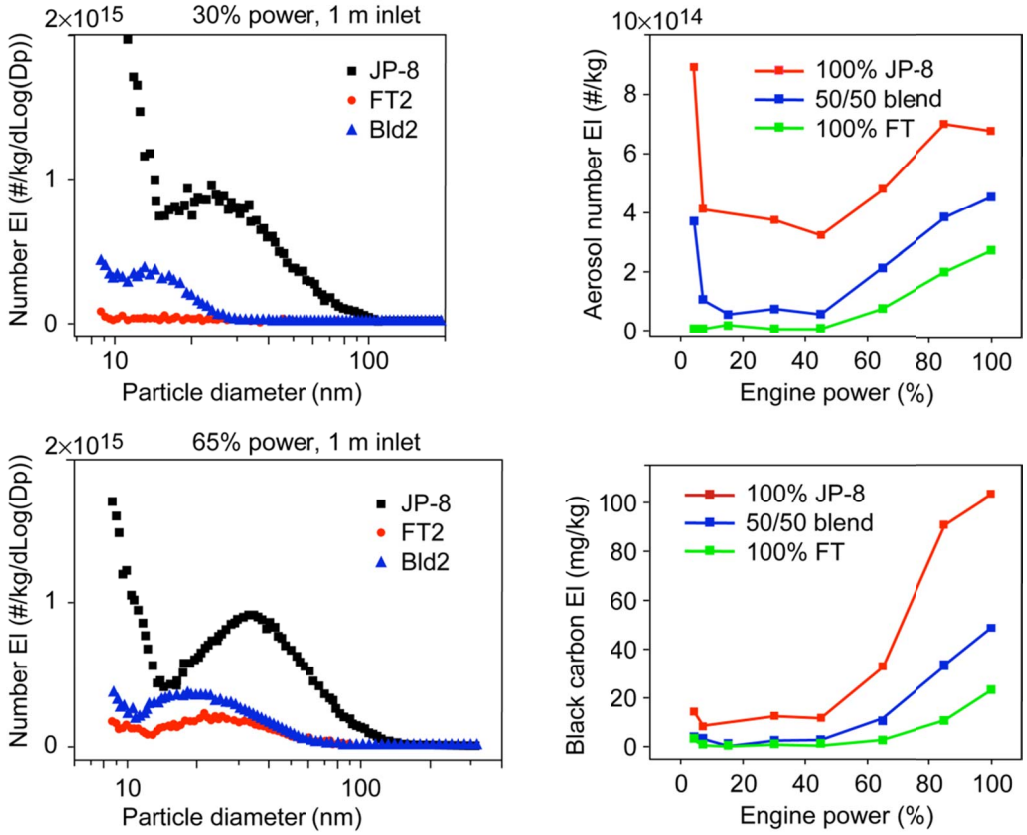

Figure 31.—On-wing engine emissions testing measurements for particulates with JP-8, 50:50 JP-8 and S8 blend, and 100% S8, where S8 represents an FT fueling with either coal- or gas-derived jet fuel, 1 meter downstream of exhaust plane (Ref. 8).

Measurement precision is much better than potential errors in measurements. For example, if most of the particles are >10 nm in size, determination of EI values in the range of (1 to 100)×10^{14}/kg fuel burned is to about 10% precision. Similarly, the "apparent" black carbon (BC) EI of between 10 and 1000 mg/(kg fuel burned) is also to about 10% precision. However, estimate of errors can be an order of magnitude greater arising from the several factors such as (Ref. 8)

1. Lack of instrument measurement specificity for black carbon(BC)
2. Lack of direct measurement approaches for BC mass
3. Lack of standards: BC characteristics vary widely between and within combustion sources
4. Severe particulate losses within sampling lines (e.g., 50% to 70% in a 25-m line prior to the diagnostic instruments)
5. Interference from background particulates, which often comprise dust and other refractory particles that do not evaporate in the combustor.

Comparisons of engine on-wing missions data (Ref. 8) and combustor-sector test data herein imply (but not conclude at this time) that sector test data replicate, at least qualitatively, on-wing test data, providing both detail and insights not gained from on-wing testing, including particulate data. Post AAFEX 2010 Workshop data (Ref. 9) also show similar qualitative emissions trends for both gaseous and particulate emissions with emissions results herein, yet elude quantitative comparisons for lack of measurement scales on many of the AAFEX reported emissions data plots.

There are qualitative differences in the emissions depending on SPK alternate fueling relative to both SPK and JP-8 fueling; however, quantitative values are not given and while these differences appear to be minor, but not insignificant, the actual values remain to be demonstrated. While this feedstock dependency of the fueling may not be large, it remains to be evaluated, which in turn affects the ASTM specifications and the presumption of being feedstock agnostic.

The EPA (Ref. 10) provided logarithmically-transformed emissions index composites data sets for three turbofan engines with selected fueling types similar to those used for AAFEX. These data show significant changes with engine and fuel type. Sixty-four semivolatile organic compounds (n-alkanes and polycyclic aromatic hydrocarbons (PAH) were measured (Ref. 10). The coupled concerns over engine and fuel type may delay FT fueling certification or prompt regulation.

It should also be noted that current aircraft auxiliary power units (APUs) (2011) have significantly higher black carbon emissions than on-wing engines (Ref. 8).

Conclusions: Part B

Alternate fueling testing is being carried out to determine preliminary performance, emissions, and particulates combustor sector data relative to JP-8+100 as baseline fueling, for SPK-type (e.g., Fischer-Tropsch, FT) fuels blends and projections for testing of biofuel fuel blends leading to preliminary development of smart fueling (fuel flexible) and combustor systems for the next generation aeronautic and aeronautic-derivative gas turbine engines. Herein alternate fueling test results for a well characterized but proprietary combustor are provided for JP-8+100, a FT-derived fuel, and a blend of 50% each by volume.

The test data presented are part of a more extensive data set where combustion parameters were varied over a range of values. The data herein are for the case of nominal inlet conditions at 75 psia (0.517 MPa) to 225 psia (1.551 MPa) and 800 °F (700 K), and JP-8+100 is taken as the baseline.

The 50:50 blend test performance and emissions results generally are between JP and FT and somewhat closer to FT

Emissions: CO is lower with FT; CO_2 is about the same; NO is lower with FT; NO_2 is higher with FT fueling F/A; NOx is lower to higher with FT with F/A; O_2 decreases with F/A (consistent with temperature increase), is lower with FT with increased spread from JP-8 with F/A, again consistent with rake temperature; HC generally decreases with F/A, yet FT humps at 0.015. No explanation is provided.

Basic emissions show more change with F/A than with JP-8 or FT; the latter being the more significant. These results appear to agree qualitatively to on-wing engine testing. Quantitative agreement requires resolution pending data release. The other aspect is to look at how emissions change with pressure and EXTRAPOLATE those results to core pressure on the ground, that is, at much higher pressures.

These comparisons and test data presented herein imply—yet at this time cannot conclude—that sector test data replicate, at least qualitatively, on-wing test data, providing both detail and insights not gained from on-wing tests. Post AAFEX 2010 Workshop analysis of released data and data herein is warranted.

Comparisons of engine on-wing test data (Ref. 8) and combustor-sector test data herein imply (but not conclude at this time) replicate, at least qualitatively, on-wing test data, for both gaseous emissions and particulate results, providing both detail and insights not gained from on-wing tests. Post AAFEX 2010 Workshop data (Ref. 9) also show similar qualitative emissions trends with results herein, yet elude quantitative comparisons for lack of scales on many of the AAFEX reported data.

SPK and JP-8 emissions profiles are qualitatively similar, yet there are observable differences in the emissions depending on alternate fueling feedstock and engine type, however quantitative AAFEX values are not provided and remain to be demonstrated. This feedstock dependency makes it more difficult for ASTM to certify as fuel feedstock agnostic and may require conformity to more strict ASTM fuel requirements?

It should also be noted that current aircraft APU's (2011) have significantly higher black carbon emissions than on-wing engines (Ref. 8).

Appendix A.—Fuel Specifications

TABLE A–1.—FUEL SPECIFICATIONS FOR FT FUEL,
AFRL NO. 5172-6: LAB REPORT 2007LA06946001

Method	Test	Result
ASTM D 3242–05	Total acid number (mg KOH/g)	0.002
ASTM D 1319–05	Aromatics (% vol)	0.0
ASTM D 3227–04a	Mercaptan sulfur (% mass)	0.000
ASTM D 4294–03	Total sulfur (% mass)	0.00
ASTM D 86–07a	Distillation Initial boiling point (°C) 10% recovered (°C) 20% recovered (°C) 50% recovered (°C) 90% recovered (°C) End point (°C) Residue (% vol) Loss (% vol)	 148 162 163 169 185 198 0.9 1.1
ASTM D 93–07	Flash point (°C)	44
ASTM D 4052–96	API gravity @ 60 °F	60.5
ASTM D 5972–05	Freezing point (°C)	–54
ASTM D 445–06	Viscosity @ –20 °C (mm^2/s)	2.6
ASTM D 3338–05	Net heat of combustion (MJ/kg)	44.2
ASTM D 3343–05	Hydrogen content (% mass)	15.6
ASTM D 1322–97	Smoke point (mm)	40.0
ASTM D 130–04	Copper strip corrosion (2h @ 100 °C)	1a
ASTM D 3241–06	Thermal stability @ 260 °C Change in pressure (mmHg) Tube deposit rating, visual	 0 1
ASTM D 381–04	Existent gum (mg/100 mL)	<1
ASTM D 5452–06	Particulate matter (mg/L)	0.5
MIL–DTL–83133E	Filtration time (min)	3
ASTM D 1094–00	Water reaction interface rating	1
ASTM D 5006–03	FSII (% vol)	0.00
ASTM D 2624–07	Conductivity (pS/m)	233
ASTM D 5001–06	Lubricity test (BOCLE) wear scar (mm)	0.77
ASTM D 4809–06	Net heat of combustion (MJ/kg)	44.2
MIL–DTL–83133E	Workmanship	Pass

TABLE A–2.—FUEL SPECIFICATIONS FOR
AFRL NO. B18-JP8+100: LAB REPORT 2009LA16176001
[ASTM-D1332 smoke point was greater than 40.00 mm.]

Method	Test	Result
ASTM D 3242–08	Total acid number (mg KOH/g)	0.003
ASTM D 1319–08	Aromatics (% vol)	18.5
ASTM D 3227–04a	Mercaptan sulfur (% mass)	0.000
ASTM D 4294–08a	Total sulfur (% mass)	0.05
ASTM D 86–08	Distillation	
	Initial boiling point (°C)	160
	10% recovered (°C)	178
	20% recovered (°C)	163
	50% recovered (°C)	203
	90% recovered (°C)	240
	End point (°C)	261
	Residue (% vol)	1.3
	Loss (% vol)	0.8
ASTM D 93–08	Flash point (°C)	46
ASTM D 4052–96	API gravity @ 60 °F	46.0
ASTM D 5972–05e1	Freezing point (°C)	–50
ASTM D 445–06	Viscosity @ –20 °C (mm^2/s)	4.2
ASTM D 3338–08	Net heat of combustion (MJ/kg)	43.3
ASTM D 3343–05	Hydrogen content (% mass)	13.8
ASTM D 1322–08	Smoke point (mm)	26.0
ASTM D 130–04	Copper strip corrosion (2h @ 100 °C)	1a
ASTM D 3241–08a	Thermal stability @ 260 °C	
	Change in pressure (mmHg)	0
	Tube deposit rating, visual	1
ASTM D 381–04	Existent gum (mg/100 mL)	4.4
ASTM D 5452–08	Particulate matter (mg/L)	0.3
MIL–DTL–83133F	Filtration time (min)	6
ASTM D 1094–00	Water reaction interface rating	-----
ASTM D 5006–03	FSII (% vol)	0.10
ASTM D 2624–07	Conductivity (pS/m)	498
ASTM D 5001–06	Lubricity test (BOCLE) wear scar (mm)	-----
ASTM D 4809–06	Net heat of combustion (MJ/kg)	-----
MIL–DTL–83133F	Workmanship	Pass

Appendix B.—Test Facility Conditions, Operations, Schematic and Fueling System

The facility test conditions were

- Pressure: 75, 125, 175, and 225 psia (0.52, 0.86, 1.21, and 1.55 MPa)
- Temperature: 500, 625, 725, and 790 °F (367, 658, and 694 K)
- Pressure drops across combustor: –3%, 4%, and 5% Δ P
- Fuel blends: 100% JP-8, 50:50, and 100% FT

The general operating procedures followed:

- Set the appropriate pressure, temperature, and combustor pressure drop (DP) with JP-8, and collect data set.
- Adjust the alternative fuel system pressure.
- Blend the alternative test fuel to the appropriate ratio based on mass flow, and collect data.
- Adjust the ratio mass flow accordingly, and collect data.

Instrumentation controls and characterization data available in testing:

- Optical access into combustion chamber
- Application of advanced laser diagnostics
- Continuous low-pressure altitude capabilities
- Application of advanced sensors for open- and closed-loop combustion control
- Characterization of advanced fuels

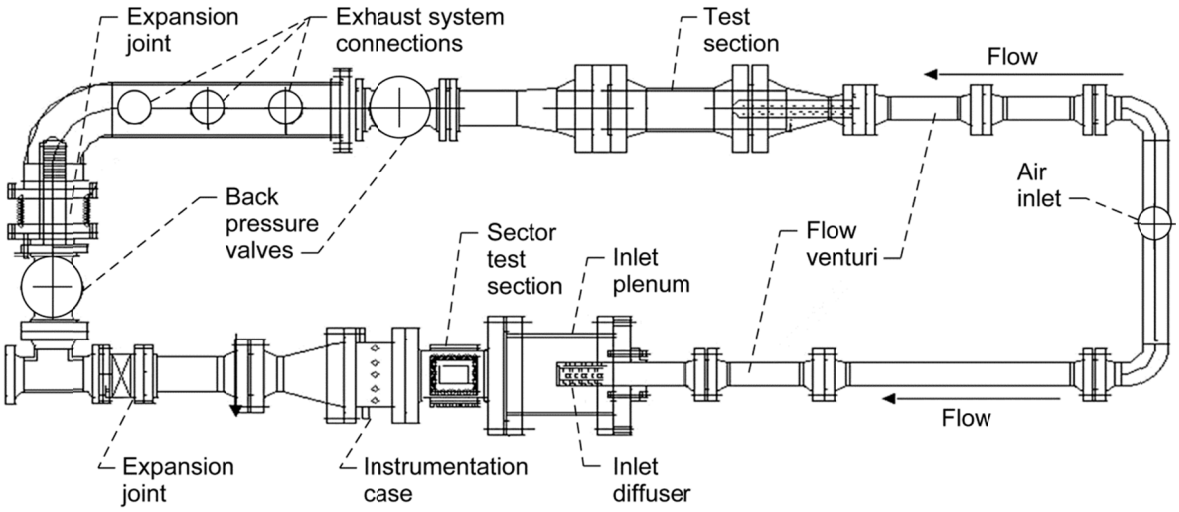

Figure B–1.—AFRL experimental test loops. The lower segment was used in the tests reported herein.

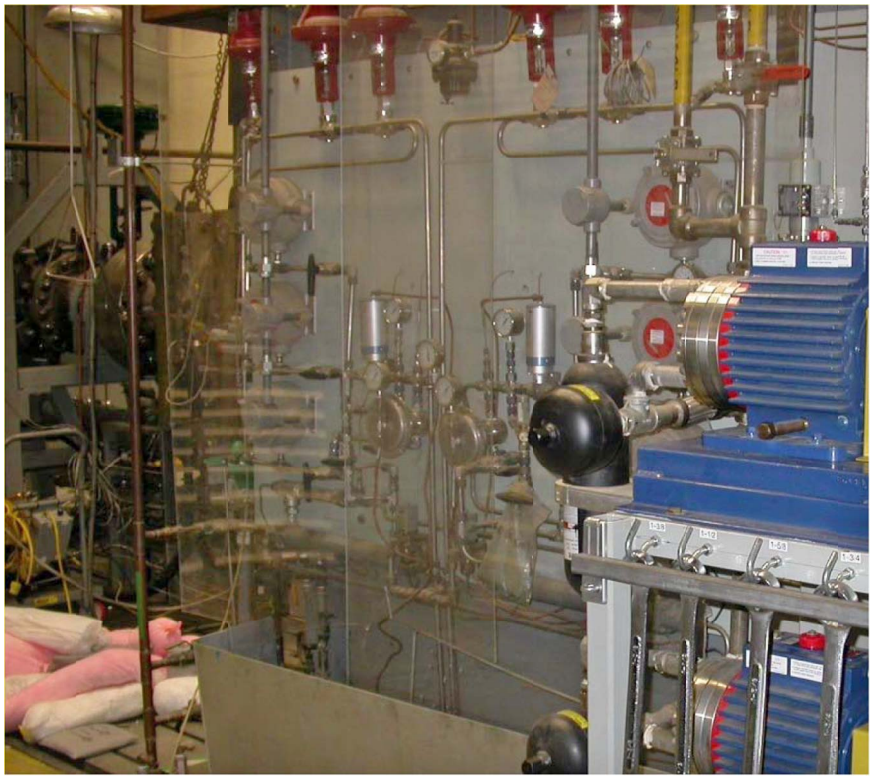

Figure B–2.—Fueling station adjacent to the test section, providing blended fueling on demand. Foreground is the main fuel pump and the secondary blending system in background.

Figure B–3.—Photos of portable alternate fueling transport and facility supply tank.

Appendix C.—Estimates of Measurement Errors

In this appendix we provide estimates of errors in the data measurements repeatability for the combustor, on-wing, and fuel blend ratios and some additional explanations for arriving at those estimates.

Combustor sector experiments

Thermal measurements: ±0.5% full scale
Flow measurements: ±1%
Fuel flow measurements (turbine flow meters ±0.25%)
Fuel blend ratio less than ±4%
Static pressure: ±0.1%
Thermal rake: ±0.5% to 3%
Emissions rake: ±1%
Relative carbon balance: ±3%
Calculated flame temperature: ±3%
Particulates: ±5% to 10%

Smoke number: ±3 SN, where SN = [(mg-C)/s] / [(kg-combustor gas)/s]

Note 1: Thermocouple geometric placement: ±1.5%.
Note 2: The relative carbon balance error involves comparison of metered experimental to calculated fuel/air ratio (F/A = FAR), determined from the emissions data [CO, CO2, HC and NOx], per SAE Aerospace Recommended Practice (ARP) 1533 guidance (Ref. 11). The emissions analyzers are calibrated prior to every day-to-day test using certified (2%) gas concentrations. The relative error is considered representative data (across industry), when it is between 10% and 15% (10% for engines above idle and 15% at idle). Herein the uncertainty in the measured raw emissions data is considered 3%, accurate to the 2% certified gas calibrations and accounting for the combined propagated error for the analyzer specifications: 1% full-scale reading. With multiple calibration gases the analyzers are accurate with the standard gas, repeatable (precise), such that the relative error in the carbon balance is considered accurate to 3%.
Note 3: The calculated flame temperature is a thermodynamic energy balance between reactants and products, utilizing emissions data (efficiency) and experimental operating conditions; it is consistent with temperatures determined from thermocouple rakes (based on multiple experiments, to within ±10 °F (±5.6 °C)), which reinforces the cited 0.5% error full scale. However, the calculated flame temperature can be no better than 3% because it is based on efficiency, as calculated from SAE ARP 1533 [11].

Estimates of error for on-wing data
gaseous emissions ±5 % or better
Black Carbon (BC) number or mass ±6 % or better
Particulates measurement variations [not repeatability (precision) error bands] can be large as there are no convenient methods for calibrating instruments. Nanoparticulates are lost on rake placement, probe inlets, transport tubing walls and vary by species (Ref. 8), with estimate of error:
EI Number [200% (dirty engine (APU) and 100% (clean engine)]
EI mass 50% to 100%

Error of estimate for fuel blend
In an analysis to verify fuel blending, samples of the 50/50 blended fuel were collected just upstream of the fuel injectors. The FT fuel used to make the JP-8+100/FT blend contained no aromatics (<0.2 volume %), so analysis of aromatic hydrocarbon content was used to determine the ratio of JP-8+100 in the JP-8+100/FT blend. The analysis was performed using ASTM D6379. In this method, normal-phase high performance liquid chromatography (HPLC) with refractive index detection was used. The aromatics

were eluted from a cyano column (4.6 × 150 cm) with hexanes as the mobile phase. Standards containing mono-aromatics and di-aromatics were used to calibrate the HPLC (Agilent Model 1100). Both standards and samples were diluted to the same level (1:50) in hexanes before injection into the HPLC. The refractive index peak areas were used to quantify the mono-aromatics and di-aromatics concentrations. These were summed to yield the total aromatics content in the fuels in volume percent. The JP-8+100 fuel sample contained 17.3 volume % aromatics and the JP-8+100/FT blend sample contained 8.3 volume % aromatics. Thus, the ratio of JP-8+100 in the blend was 8.3/17.3 or 0.48, or 48% JP-8+100 and 52% FT to within 4%.

Appendix D.—Combustor Thermal Data and Post Processing Parameters

TABLE D–1.—COMBUSTOR OUTER AND INNER LINER TEMPERATURE, THERMAL DIFFERENCE DATA, AND NUMBER AND NAME OF THERMOCOUPLES (TCS) USED TO PLOT THERMAL PROFILES.[a,b,c]

				F/A = 0.010			F/A = 0.015			F/A = 0.020		
TC	Unwrapped[d]			JP-8	FT	50:50	JP-8	FT	50:50	JP-8	FT	50:50
	TC No.	X	Θ	Col C	Col G	Col F	Col O	Col K	Col M	Col Q	Col V	Col T
Outer liner												
			0.00									
TOLAL	22	0.94	0.20	817	825	825	852	850	846	882	873	881
TOLFL	20	0.00	0.22	900	904	907	968	935	946	1030	971	1002
TOLML	21	0.67	0.26	861	870	869	927	924	925	987	957	985
TOLMWA	24	0.19	0.32	870	875	878	962	917	944	1027	960	1002
TOLFM	27	0.00	0.34	899	902	908	983	944	956	1060	985	1024
TOLCA	25	1.00	0.52	862	872	872	920	910	912	986	952	974
TOLAM	28	0.94	0.58	814	825	825	852	851	850	888	874	886
TOLMR	36	0.67	0.62	873	887	884	953	918	941	1013	955	996
TOLFR	34	0.00	0.74	887	888	891	965	924	944	1016	956	1001
TOLMWI	23	0.33	0.79	879	879	884	933	905	914	992	937	969
TOLAR	37	0.84	0.86	831	843	843	877	872	874	917	906	922
TSWFD	41	0.22	0.97	1218	1288	1280	1438	1469	1444	1544	1565	1581
TSWFT	30	0.78	1.00	814	820	820	847	836	841	854	842	850
Inner liner												
TILMWI	38	0.50	1.20	897	908	906	994	969	976	1091	1023	1066
TILFR	35	0.00	1.23	890	917	919	995	959	967	1075	1006	1050
TILMWO	26	0.50	1.33	902	908	909	988	962	968	1096	1025	1071
TILCA	29	1.00	1.50	1056	1065	1058	1229	1217	1219	1411	1326	1348
TILFL	39	0.00	1.54	913	917	916	1002	970	981	1098	1030	1069
			2.00									

[a]Geometric position accuracy of thermocouple position coordinates is estimated at ±1.5%.

[b]For nominal inlet pressure 225 psia (1.55 MPa), 800 °F (700 K), and 3% combustor pressure drop.

[c]Note: Col C, G, F, K, M, Q, V, and T are data set tracking identifiers.

[d]X = x/L (which varies from 0 to 1), where x is the TC position measured from the liner inlet and L is the overall liner length.

Θ = circumferential TC position measured over the liner outside y/L_θ (0 to 1) and continuing back along the inside liner (1 to 2), where L_θ is half the unwrapped liner "width." The normalized unwrapped coordinate (X, Θ) is the TC location (x, y)

TABLE D–2.—COMBUSTOR OUTER AND INNER LINER TEMPERATURE DIFFERENCE WITH RESPECT TO JP-8+100[a] ($T_{FUEL\ BLEND} - T_{JP-8}$) (°F)

[For nominal inlet pressure 225 psia (1.55 MPa), 800 °F (700 K), and 3% combustor pressure drop.]

				F/A = 0.010			F/A = 0.015			F/A = 0.020		
TC	Unwrapped[c]			JP-8	FT	50:50	JP-8	FT	50:50	JP-8	FT	50:50
	TC No.	X	Θ	Col C	Col G	Col F	Col O	Col K	Col M	Col Q	Col V	Col T
Outer liner												
Circumferential start point			0.00									
TOLAL	22	0.94	0.20	0	8	8	0	–2	–6	0	–9	——
TOLFL	20	0.00	0.22	0	4	7	0	–33	–22	0	–1	–28
TOLML	21	0.67	0.26	0	9	8	0	–3	–2	0	–30	–2
TOLMWA	24	0.19	0.32	0	5	8	0	–45	–18	0	–67	–25
TOLFM	27	0.00	0.34	0	3	9	0	–39	–2	0	–75	–36
TOLCA	25	1.00	0.52	0	10	10	0	–10	–8	0	–34	–12
TOLAM	28	0.94	0.58	0	11	11	0	–1	–2	0	–14	–2
TOLMR	36	0.67	0.62	0	14	11	0	–35	–12	0	–58	–17
TOLFR	34	0.00	0.74	0	1	4	0	–41	–21	0	–60	–15
TOLMWI	23	0.33	0.79	0	0	5	0	–28	–19	0	–55	–23
TOLAR	37	0.84	0.86	0	12	12	0	–5	–3	0	–11	5
TSWFD	41	0.22	0.97	0	70	62	0	31	6	0	21	37
TSWFT	30	0.78	1.00	0	6	6	0	–11	–6	0	–12	–4
Inner liner												
TILMWI	38	0.50	1.20	0	11	9	0	–25	–18	0	–68	–25
TILFR	35	0.00	1.23	0	27	29	0	–36	–28	0	–69	–25
TILMWO	26	0.50	1.33	0	6	7	0	–26	–20	0	–71	–25
TILCA	29	1.00	1.50	0	9	2	0	–12	–10	0	–85	–63
TILFL	39	0.00	1.54	0	4	3	0	–32	–21	0	–68	–29
Circumferential end point			2.00									
Average without TSWFD					8	9		–23	–14		–50	–19
Average with TSWFD					12	12		–20	–13		–46	–16
Average $\left(\frac{\text{without + with}}{2}\right)$					10	10		–21	–14		–48	–18

[a]Geometric position accuracy of thermocouple position coordinates is estimated at ±1.5%.

[b]Note $\Delta°C = \Delta K = \Delta°F/1.8$.

[c]X = x/L where x is the TC position measured from the liner inlet and L_x is the overall liner length.

Θ = circumferential TC position measured over the liner outside/L_θ (0 to 1) and continuing back along inside liner (1 to 2) where L_θ is half the unwrapped liner "width."

Thermocouple number and name used in plotting thermal and thermal difference profiles. These selected TCs provide for nominal axial and circumferential thermal and differential thermal profiles. The profiles are not aligned with mutually perpendicular coordinate locations.

TABLE D–3.—THERMOCOUPLE (TC) NUMBER AND NAME USED IN PLOTTING THERMAL AND THERMAL DIFFERENCE PROFILES[a]

Liner outer wall							
Axial		Circumferential					
		Forward (FWD)		Midplane (MID)		Aft (AFT)	
TC No.	TC name	TC No.	TC name	TC No.	TC name	TC No.	TC name
20	TOLFL	20	TOLFL	21	TOLML	22	TOTAL
27	TOLFM	27	TOLFM	24	TOLMWA	25	TOLCA
24	TOLMWA	34	TOLFR	36	TOLMR	28	TOLAM
21	TOLML			23	TOLMWI	37	TOLAR
22	TOLAL						
Liner inner wall							
Axial		Circumferential					
		Forward (FWD)		Midplane (MID)		Aft (AFT)	
TC No.	TC name	TC No.	TC name	TC No.	TC name	TC No.	TC name
35	TILFR	35	TILFR	38	TILMLWI	29	TILCA
26	TILMWD	39	TILFL	36	TILMWD		
29	TILCA						

[a]These selected TCs provide for nominal axial and circumferential thermal and differential thermal profiles. The profiles are not aligned with mutually perpendicular coordinate locations.

References

1. Hendricks, R.C., Shouse, D.T., Roquemore, W.M., Burns, D.L., Duncan, B.S., Ryder, R.C., Brankovic, A., Liu, N.-S, Gallagher, J.R., and Hendricks, J.A., 2004, "Experimental and Computational Study of Trapped Vortex Combustor Sector Rig With Tri-Pass Diffuser," NASA/TM—2004-212507, NASA Glenn Research Center, Cleveland, OH.
2. Shouse, D.T., Stutrud, J.S., and Frayne, C.W., 2001, "High Pressure Combustion Research at the Air Force Research Laboratory," ISABE–2001–1119, Fifteenth International Symposium on Air Breathing Engines, Bangalore, India.
3. Ryder, R.C., Hendricks, R.C., Huber, M.L., and Shouse, D.T., 2010, "Computational Analysis of Dynamic SPK(S8)-JP-8 Fueled Combustor-Sector Performance," submitted to Journal of Engineering for Gas Turbines and Power.
4. Kinder, J.D., and Rahmes, T., 2009, "Evaluation of Bio-Derived Synthetic Paraffinic Kerosenes (Bio-SPK)," Sustainable Biofuels Research & Technology Program document, The Boeing Company, Seattle, WA. http://www.boeing.com/aboutus/govt_ops/reports_white_papers/pas_biofuel_exec_summary.pdf
5. Bulzan, D., 2009, "Alternative Aviation Fuel Experiment (AAFEX): Overview," NASA Glenn Research Center, Cleveland, OH.
6. NASA, AFRL, ARI, UTRC, and P&W, 2008, "Alternative Fuel Test on PW308 Engine," collaborative presentation.
7. Rahmes, T.F., Kinder, J.D., Henry, T.M., Crenfeldt, G., LeDuc, G.F., Zombanakis, G.P., Abe, Y., Lambert, D.M., Lewis, C., Juneger. J.A., Andac, M.G., Reilly, K.R., Holmgren, J.R., McCall, M.J., and Bozzano, A.G., 2009, "Sustainable Bio-Derived Synthetic Paraffinic Kerosene (Bio-SPK) Jet Fuel Flights and Engine Tests Program Results," AIAA 2009–7002, *9th AIAA Aviation Technology, Integration, and Operation Conference (ATIO)*, AIAA, Reston, VA.
8. Anderson, B., 2009, "Langley Aircraft Emission Research: Highlights and Overview of the Alternative Aviation Fuel Experiment," AMRD/AAFEX program presentation, NASA Langley Research Center, Hampton, VA.
9. Bulzan, D. et al. (15 authors), 2010, "Gaseous and Particulate Emissions Results of the NASA Alternate Aviation Fuel Experiment (AAFEX)," GT2010-23524, Proceedings of ASME Turbo Expo 2010: Power for Land, Sea and Air GT2010 June 14-18, 2010 Glasgow, Scotland.
10. Kinsey, J.S., Hays, M.D., Don, Y., Williams, D.C., and Logan, R., 2011, "Chemical Characterization of the Fine Particle Emissions from Commercial Aircraft Engines during the Aircraft Particle Emissions eXperiment (APEX) 1 to 3," Environmental Science Technology, 23 March 2011, http://pubs.acs.org/doi/abs/10.1021/es103880d.
11. SAE International, 2004, "Procedure for the Analysis and Evaluation of Gaseous Emissions from Aircraft Engines," Aerospace Recommended Practice 1533A.

REPORT DOCUMENTATION PAGE		Form Approved OMB No. 0704-0188

1. REPORT DATE *(DD-MM-YYYY)*	2. REPORT TYPE	3. DATES COVERED *(From - To)*
01-07-2012	Technical Memorandum	

4. TITLE AND SUBTITLE
Alternate-Fueled Combustor-Sector Performance
Part A: Combustor Performance
Part B: Combustor Emissions

5a. CONTRACT NUMBER

5b. GRANT NUMBER

5c. PROGRAM ELEMENT NUMBER

6. AUTHOR(S)
Shouse, D., T.; Neuroth, C.; Hendricks, R., C.; Lynch, A.; Frayne, C., W.; Stutrud, J., S.; Corporan, E.; Hankins, Capt., T.

5d. PROJECT NUMBER

5e. TASK NUMBER

5f. WORK UNIT NUMBER
WBS 561581.02.08.03.16.03

7. PERFORMING ORGANIZATION NAME(S) AND ADDRESS(ES)
National Aeronautics and Space Administration
John H. Glenn Research Center at Lewis Field
Cleveland, Ohio 44135-3191

8. PERFORMING ORGANIZATION REPORT NUMBER
E-17205-2

9. SPONSORING/MONITORING AGENCY NAME(S) AND ADDRESS(ES)
National Aeronautics and Space Administration
Washington, DC 20546-0001

10. SPONSORING/MONITOR'S ACRONYM(S)
NASA

11. SPONSORING/MONITORING REPORT NUMBER
NASA/TM-2012-217128

12. DISTRIBUTION/AVAILABILITY STATEMENT
Unclassified-Unlimited
Subject Categories: 03, 05, 07, and 44
Available electronically at http://www.sti.nasa.gov
This publication is available from the NASA Center for AeroSpace Information, 443-757-5802

13. SUPPLEMENTARY NOTES

14. ABSTRACT

Alternate aviation fuels for military or commercial use are required to satisfy MIL-DTL-83133F(2008) or ASTM D 7566 (2010) standards, respectively, and are classified as “drop-in” fuel replacements. To satisfy legacy issues, blends to 50% alternate fuel with petroleum fuels are certified individually on the basis of processing and assumed to be feedstock agnostic. Adherence to alternate fuels and fuel blends requires “smart fueling systems” or advanced fuel-flexible systems, including combustors and engines, without significant sacrifice in performance or emissions requirements. This paper provides preliminary performance (Part A) and emissions and particulates (Part B) combustor sector data. The data are for nominal inlet conditions at 225 psia and 800 °F (1.551 MPa and 700 K), for synthetic-paraffinic-kerosene- (SPK-) type (Fisher-Tropsch (FT)) fuel and blends with JP-8+100 relative to JP-8+100 as baseline fueling. Assessments are made of the change in combustor efficiency, wall temperatures, emissions, and luminosity with SPK of 0%, 50%, and 100% fueling composition at 3% combustor pressure drop. The performance results (Part A) indicate no quantifiable differences in combustor efficiency, a general trend to lower liner and higher core flow temperatures with increased FT fuel blends. In general, emissions data (Part B) show little differences, but with percent increase in FT-SPK-type fueling, particulate emissions and wall temperatures are less than with baseline JP-8. High-speed photography illustrates both luminosity and combustor dynamic flame characteristics.

15. SUBJECT TERMS
Combustors; Engines; Fuels; Environment; Testing

16. SECURITY CLASSIFICATION OF:			17. LIMITATION OF ABSTRACT	18. NUMBER OF PAGES	19a. NAME OF RESPONSIBLE PERSON
a. REPORT	b. ABSTRACT	c. THIS PAGE			STI Help Desk (email:help@sti.nasa.gov)
U	U	U	UU	49	19b. TELEPHONE NUMBER *(include area code)* 443-757-5802